Functional genomics of epilepsy-associated mutations in the $GABA_A$ receptor subunits reveal that one mutation impairs function and two are catastrophic

Received for publication, September 3, 2018, and in revised form, January 30, 2019 Published, Papers in Press, February 6, 2019, DOI 10.1074/jbc.RA118.005697

Nathan L. Absalom[‡§], Philip K. Ahring[‡§], Vivian W. Liao[‡§], Thomas Balle[‡§], Tian Jiang[‡§], Lyndsey L. Anderson[‡¶‖], Jonathon C. Arnold[‡¶‖], Iain S. McGregor[‡‖], Michael T. Bowen[‡‖**], and Mary Chebib[‡§1]**

From the [‡]Brain and Mind Centre and [‖]Lambert Initiative for Cannabinoid Therapeutics, University of Sydney, 94 Mallett Street, Camperdown, New South Wales 2050, Australia and the [§]School of Pharmacy and [¶]Discipline of Pharmacology, Faculty of Medicine and Health, and the [**]School of Psychology, Faculty of Science, University of Sydney, Camperdown, New South Wales 2006, Australia

Edited by Mike Shipston

A number of epilepsy-causing mutations have recently been identified in the genes of the α1, β3, and γ2 subunits comprising the γ-aminobutyric acid type A ($GABA_A$) receptor. These mutations are typically dominant, and in certain cases, such as the α1 and β3 subunits, they may lead to a mix of receptors at the cell surface that contain no mutant subunits, a single mutated subunit, or two mutated subunits. To determine the effects of mutations in a single subunit or in two subunits on receptor activation, we created a concatenated protein assembly that links all five subunits of the $\alpha1\beta3\gamma2$ receptor and expresses them in the correct orientation. We created nine separate receptor variants with a single-mutant subunit and four receptors containing two subunits of the $\gamma2^{R323Q}$, $\beta3^{D120N}$, $\beta3^{T157M}$, $\beta3^{Y302C}$, and $\beta3^{S254F}$ epilepsy-causing mutations. We found that the singly mutated $\gamma2^{R323Q}$ subunit impairs GABA activation of the receptor by reducing GABA potency. A single $\beta3^{D120N}$, $\beta3^{T157M}$, or $\beta3^{Y302C}$ mutation also substantially impaired receptor activation, and two copies of these mutants within a receptor were catastrophic. Of note, an effect of the $\beta3^{S254F}$ mutation on GABA potency depended on the location of this mutant subunit within the receptor, possibly because of the membrane environment surrounding the transmembrane region of the receptor. Our results highlight that precise functional genomic analyses of $GABA_A$ receptor mutations using concatenated constructs can identify receptors with an intermediate phenotype that contribute to epileptic phenotypes and that are potential drug targets for precision medicine approaches.

Epileptic encephalopathies are a devastating group of severe childhood epilepsies with poor developmental outcomes that are often resistant to pharmacological treatment (1). In many cases, the causes are genetic, and recent advances in whole-genome sequencing have identified a series of *de novo* and inherited mutations in various genes. Several mutations in genes that encode for the α1 (2–9), β3 (4, 7, 8, 10–12), and γ2 subunits (4, 7, 9, 13–16) of the GABA type A ($GABA_A$)[2] receptor (*GABRA1*, *GABRB3*, and *GABRG2*, respectively) have been identified that result in epileptic encephalopathies.

$GABA_A$ receptors are essential mediators of neurotransmission in both the developing and adult brain (17). These receptors are ion channels composed of five subunits that arrange around a central ion pore (18). When GABA is released from the synapse, it binds to these receptors anchored at the postsynaptic membrane to open an ion channel, allowing chloride ions to pass, hyperpolarizing and inhibiting the cell (19).

Many genes encoding for different subunits of the $GABA_A$ receptor are present in the mammalian brain, including six α (α1–6), three β (β1–3), three γ (γ1–3), and a δ, ϵ, and π, and the majority of receptors are thought to contain two α, two β, and one γ subunit where they are anchored at the synapse, responding to high concentrations of GABA (20). Other combinations of receptors, often containing δ subunits, are found extrasynaptically, where they respond to low concentrations of GABA or spillover from the synapse (21). Each individual subunit consists of a large extracellular domain, four transmembrane domains where the second (M2) lines the channel pore, two short and one large loop linking transmembrane domains, and a short C terminus. At synaptic receptors, GABA binds within the β–α interface located between adjacent extracellular domains to trigger an activation pathway through a series of conformational changes that ultimately open the channel pore. These conformational changes are transmitted through interactions at the coupling region, where loops in the extracellular domain in close proximity to the membrane interact with the pre-M1 and M2-M3 loops that connect transmembrane domains (22). This results in tilt of the M2 domain to open the pore. Epilepsy-causing mutations identified in the α1, β3, and γ2 subunits are located at different regions throughout the protein, including amino acids throughout the activation pathway from the ligand-binding pocket and extracellular structural β-sheets, through to the coupling and transmembrane M1 and M2 regions.

This work was supported by the Lambert Initiative and by National Health and Medical Research Council Grants APP1124567 and APP1081733. The authors declare that they have no conflicts of interest with the contents of this article.

This article contains Fig. S1.

[1] To whom correspondence should be addressed: Brain and Mind Centre, University of Sydney, 94 Mallett St., Camperdown, New South Wales 2050, Australia. Tel.: 612-9351-8584; Fax: 612-9351-4391; E-mail: mary.collins@sydney.edu.au.

[2] The abbreviations used are: $GABA_A$, γ-aminobutyric acid type A; cRNA, complementary RNA; Est. $P_{o(max)}$, estimated maximum open probability; cryo-EM, cryogenic EM; ANOVA, analysis of variance; PDB, Protein Data Bank.

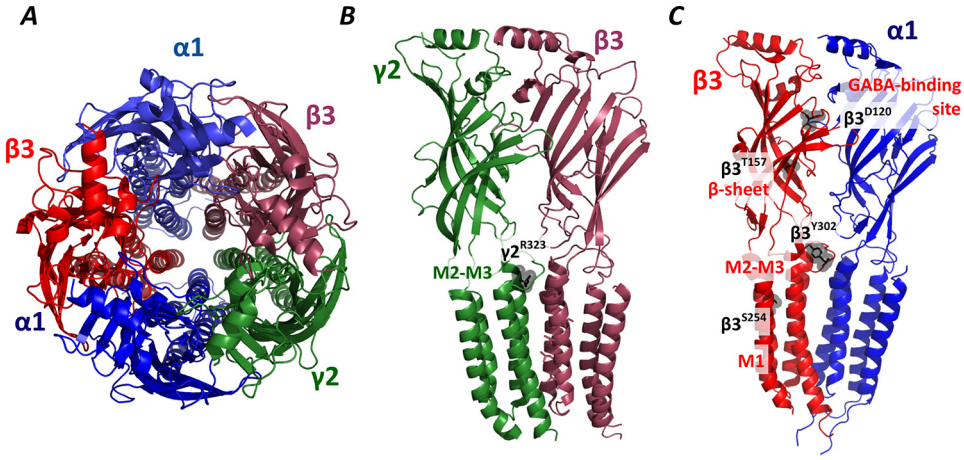

Figure 1. *A*, pentameric structure of the GABA and diazepam-bound $\alpha1\beta3\gamma2$ receptor (PDB code 6HUP) from above showing the orientation of the subunits. The subunits are *colored* with respect to their order in the pentamer: first $\gamma2$ (*green*), second $\beta3$ (*maroon*), third $\alpha1$ (*blue*), fourth $\beta3$ (*red*), and fifth $\alpha1$ (*dark blue*). *B*, *side view* showing the first $\gamma2$ subunit adjacent to the second $\beta3$ subunit. The $\gamma2^{R323}$ residue on the M2-M3 loop is depicted with the side chain in *black* in a *transparent sphere*. *C*, *side view* showing the fourth $\beta3$ subunit adjacent to the fifth $\alpha1$ subunit, with the GABA-binding site *highlighted*. The side chains of the $\beta3^{D120N}$ residue at the GABA-binding site, the $\beta3^{T157M}$ residue within an internal β-sheet, the $\beta3^{Y302C}$ residue in the M2-M3 loop, and the $\beta3^{S254F}$ residue in the M1 region are shown in *black*.

Mutations in the GABA$_A$ receptor that cause epilepsy typically impair this process, either through misfolding of protein to reduce the number of receptors at the cell surface or disturbing the ability of the receptor to open in response to GABA (8). In all cases, the mutations that cause epileptic encephalopathies are dominant, with patients carrying one copy of the WT allele and one copy of the mutant allele (2–16). For mutations in the $\gamma2$ subunit, the resultant receptors will either be a WT or contain a single mutation. However, for $\beta3$ mutations, a more complicated mixture of receptors will be expressed. A WT containing two normal $\beta3$ subunits, two heteromutant receptors containing a single mutation at either of the two $\beta3$ subunit locations within the pentamer, and a homomutant receptor containing the mutation at both $\beta3$ subunit locations within the pentamer can be formed. If the surface expression is unaffected and the distribution of mutant receptors into the complex is random, some 50% of the resultant receptors will contain mutations with just a single copy of the mutation. To date, there is a lack of research that assesses the effect of a single copy of the mutation on GABA$_A$ receptor function, an important component that contributes to understanding the epilepsy phenotype of individuals. Therefore, it is vital to determine how single copies of the mutation, as well as two copies, alter the function of the receptor to properly characterize the molecular phenotype of the mutation.

We chose five mutations to investigate using the concatenated construct including one in the $\gamma2$ subunit ($\gamma2^{R323Q}$) and four in the $\beta3$ subunit ($\beta3^{D120N}$, $\beta3^{T157M}$, $\beta3^{S254F}$, and $\beta3^{Y302C}$) (Fig. 1*A*). These mutations were chosen as they were located in different regions along the activation pathway of the receptor, including the M2-M3 coupling loop of the $\gamma2$ subunit ($\gamma2^{R323Q}$). The $\beta3$ mutations were located in the area surrounding the ligand-binding site ($\beta3^{D120N}$), a β-sheet within the extracellular domain ($\beta3^{T157M}$), the M2-M3 coupling loop ($\beta3^{Y302C}$), and the M1 transmembrane region ($\beta3^{S254F}$) (Fig. 1, *B* and *C*). Previous functional genomic analysis of these mutations in *Xenopus* oocytes and HEK293 cells have demonstrated that the $\gamma2^{R323Q}$, $\beta3^{D120N}$, and $\beta3^{Y302C}$ mutations substantially reduce either the potency of GABA or the magnitude of GABA-activated currents when expressed in $\alpha1\beta3\gamma2$ or $\alpha5\beta3\gamma3$ receptors (8, 11, 15), whereas the $\beta3^{T157M}$ mutation caused only subtle changes at $\alpha5\beta3\gamma3$ receptors (8). However, these experiments did not fully describe the molecular phenotype of the mutations, as they were unable to distinguish how receptors that contain one or two copies of the mutation differ from the WT receptor or from each other.

To resolve this question, we created a concatenated $\alpha1\beta3\gamma2$ GABA$_A$ receptor construct with five linked subunits in the sequence $\gamma2$-$\beta3$-$\alpha1$-$\beta3$-$\alpha1$. For each mutation, we then created a set of receptor constructs that resembled the expressed receptors from an individual with a dominant mutation. Typically, but not always, a single copy of the mutation impaired the activation properties of the receptor, whereas a second copy intensified the effect of the mutation to be catastrophic.

We propose that precise functional genomic analysis using concatenated receptors can identify the phenotype of the individual receptors that are expressed by patients with dominant mutations. This information may ultimately assist in precision medicine approaches, where mutant GABA$_A$ receptors containing a single mutation can be targeted to treat individual patients.

Results

Activation properties of WT concatenated receptor

To determine how receptors with either a single or two copies of an epilepsy-causing mutation differ from WT receptors, we created a concatenated receptor construct with five subunits linked by AGS repeats (Fig. 2*A*). Although concatenated ligand-gated ion channels have previously been created, many of these do not reliably form in the standard orientation (23) or are mixtures of dimeric and trimeric concatenated constructs (24). When injected alone, these dimeric and trimeric constructs can result in low currents that could potentially confound the analysis of mutations that impair receptor function (25). However, constructs of concatenated pentameric GABA$_A$

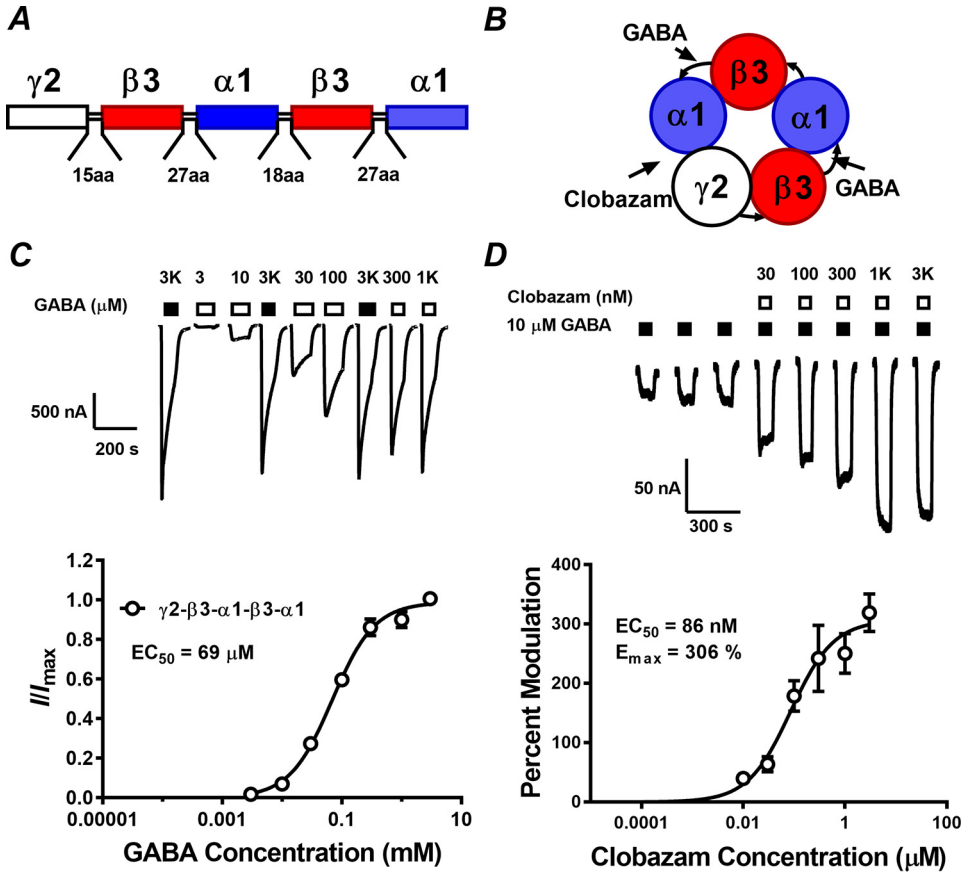

Figure 2. *A*, *schematic* of the coding region of concatenated receptor containing the DNA construct. Linker lengths are 15 amino acids ($(AGS)_5$), 27 amino acids ($(AGS)_5LGS(AGS)_3$), 18 amino acids ($AGT(AGS)_5$), and 27 amino acids ($(AGS)_4AGT(AGS)_4$). *B*, *schematic* of the expected arrangement of the concatenated receptor where the subunits arrange in a counter-clockwise orientation. GABA- and clobazam-binding sites are shown. *C*, representative data (*above*) from a single two-electrode voltage clamp experiment where different concentrations of GABA (*open bars*) were applied to construct a concentration–response curve to GABA (*below*). *Filled bars*, reference 3 mM GABA applications; *open bars*, GABA applications at concentrations shown. Peak currents were measured, and the mean ± S.E. (*error bars*) was plotted (*open circles*) and fitted to the Hill equation (*below*). *D*, representative data (*above*) from a single two-electrode voltage clamp experiment constructing a modulation curve to clobazam (*below*). Three pulses of reference 10 μM GABA (*closed bars*) were applied prior to co-application of 10 μM GABA and clobazam at concentrations shown (*closed bars*). Percent modulation of the control GABA response was calculated, and the mean ± S.E. was plotted and fitted to the Hill equation (*below*). The fitted EC_{50} of clobazam was 86 nM (log EC_{50} = −4.03 ± 0.06, mean ± S.E., n = 10), and the fitted E_{max} was 306% (320 ± 32, mean ± S.E., n = 10).

receptors have also been described that contain β2 subunits (26). Therefore, the new construct was designed with five subunits in the same order so that the subunits would arrange themselves primarily counter-clockwise when viewed from the extracellular side of the membrane, forming two GABA-binding sites at the β3-α1 interfaces and a benzodiazepine-binding site at the α1–γ2 interface (Fig. 2*B*). Sequence encoding for the signal peptide of the α1 and β3 subunits were removed, and four different linkers were incorporated with lengths calculated with the same methodology as previously (23). To ensure predominately counter-clockwise expression, the first linker was designed to be relatively short, and subsequent linkers were longer with similar lengths when N and C termini were taken into account. These linkers contained peptide sequences of $(AGS)_5$ between the γ2 and β3 subunits ($(AGS)_5LGS(AGS)_3$ between the first β3 and α1 subunits, $AGT(AGS)_5$ between the α1 and β3 subunits, and $(AGS)_4ATG(AGS)_4$ between the final β3 and α1 subunits) to form the DNA construct encoding the five subunits in the order of γ2-β3-α1-β3-α1 (Fig. 2, *A* and *B*).

cRNA (2 ng) of the WT concatenated construct was injected into *Xenopus* oocytes, and the oocytes were incubated for 2–4 days. Denaturing agarose gel electrophoresis was performed on the RNA to ensure that a single band at the correct size only was transcribed, and Western blotting was performed to ensure that the protein was properly translated and degradation products were not observed (Fig. S1). Peak currents were measured using two-electrode voltage clamp electrophysiology upon application of a range of GABA solutions, and the measured responses were used to construct the concentration–response curve (Fig. 2*C*). Injection of the WT cRNA resulted in robust GABA-activated currents, with 3 mM GABA eliciting an average current of 2 μA (Fig. 2*C* and Table 1). GABA activated the WT concatemer with an EC_{50} of 69 μM, similar to our previously published value of 53 μM and other previously published reports (*e.g.* 74 μM (27)) where unlinked α1, β3, and γ2 subunits were injected into *Xenopus* oocytes (28).

To ensure that the receptors were arranging in the correct orientation, the modulation of GABA-elicited currents of our concatenated receptors was measured using a benzodiazepine, clobazam, that binds selectively to the α1–γ2 inter-

Table 1
Concentration–response curves of $\alpha1\beta3\gamma2$ receptors
Results shown are mean ± S.E. *, $p < 0.05$; **, $p < 0.01$; ***, $p < 0.001$; one-way ANOVA with Tukey's post hoc test.

Construct	EC_{50} μM (log EC_{50})	I_3 mM_GABA	n_H	*n*	Est. $P_{o(max)}$	*n*
		nA				
γ2-β3-α1-β3-α1	69.0 (−4.12 ± 0.06)	2095 ± 126	1.3 ± 0.1	13	0.95 ± 0.04	10
$\gamma2^{R323Q}$-β3-α1-β3-α1	315 (−3.42 ± 0.04)***	1395 ± 214	0.9 ± 0.1***	10	0.85 ± 0.03	10
γ2-$\beta3^{D120N}$-α1-β3-α1	1144 (−2.77 ± 0.05)***	701 ± 92***	1.1 ± 0.1	10	1.12 ± 0.07	10
γ2-$\beta3^{T157M}$-α1-β3-α1	422 (−3.37 ± 0.05)***	1146 ± 210*	1.2 ± 0.1	10	0.90 ± 0.05	10
γ2-$\beta3^{S254F}$-α1-β3-α1	181 (−3.68 ± 0.04)***	1230 ± 134*	1.3 ± 0.1	10	1.00 ± 0.04	10
γ2-$\beta3^{Y302C}$-α1-β3-α1	164 (−3.71 ± 0.05)***	1826 ± 165	1.0 ± 0.1*	10	0.40 ± 0.06***	10
γ2-β3-α1-$\beta3^{D120N}$-α1	1473 (−2.87 ± 0.11)***	969 ± 158***	0.8 ± 0.1***	10	1.00 ± 0.05	10
γ2-β3-α1-$\beta3^{T157M}$-α1	279 (−3.53 ± 0.06)***	1995 ± 256	1.1 ± 0.1	10	0.96 ± 0.04	10
γ2-β3-α1-$\beta3^{S254F}$-α1	34.2 (−4.47 ± 0.07)**	2480 ± 248	1.2 ± 0.1	10	0.95 ± 0.03	10
γ2-β3-α1-$\beta3^{Y302C}$-α1	471 (−3.35 ± 0.09)***	1336 ± 156*	1.1 ± 0.1*	10	0.74 ± 0.05*	10
γ2-$\beta3^{D120N}$-α1-$\beta3^{D120N}$-α1	ND[a]	ND	ND	10	ND	
γ2-$\beta3^{T157M}$-α1-$\beta3^{T157M}$-α1	ND	ND	ND	10	ND	
γ2-$\beta3^{S254F}$-α1-$\beta3^{S254F}$-α1	29.6 (−4.52 ± 0.05)***	1528 ± 210	1.3 ± 0.1	10	0.89 ± 0.03	10
γ2-$\beta3^{Y302C}$-α1-$\beta3^{Y302C}$-α1	6806 (−2.16 ± 0.08)***	77 ± 15***	0.9 ± 0.1***	10	0.24 ± 0.04***	10

[a] ND, currents too low to determine concentration–response curve.

faces. When clobazam was co-applied with 10 μM GABA, the response of the activated receptors was increased with increasing clobazam concentrations (Fig. 2*D*). We constructed a concentration–response curve of clobazam modulation of 10 μM GABA-activated currents. The maximum modulation by clobazam was 306%, and the EC_{50} value of clobazam was 86 nM, similar to previously published values of 256% and 132 nM at nonconcatenated $\alpha1\beta2\gamma2$ receptors (29) (Fig. 2*D*). Taken together, the GABA and clobazam concentration–response curves demonstrate that the concatenated receptor reliably replicates the activation properties of its respective unlinked receptor. We then used this construct as a backbone so that mutant β3 and/or γ2 subunit(s) can be inserted at specific regions of the pentameric construct to analyze the effects of epilepsy-causing mutations. For γ2 mutations, a single copy of the mutation was inserted into the receptor, and for β3 mutations, either a single copy of the mutation was inserted within different subunits or two copies of the mutation were inserted into the receptor.

Absolute expression levels of mutant receptors

We chose five mutations to investigate using concatemers, including one in the γ2 subunit ($\gamma2^{R323Q}$) and four in the β3 subunit ($\beta3^{D120N}$, $\beta3^{T157M}$, $\beta3^{S254F}$, and $\beta3^{Y302C}$). These mutations were chosen as they are located in different regions along the activation pathway of the receptor. In order from the extracellular to transmembrane domains, the amino acids included the area surrounding the ligand-binding site ($\beta3^{D120N}$), a β-sheet located in the extracellular domain of the β3 subunit ($\beta3^{T157M}$), the M2-M3 coupling loop of both the γ2 ($\gamma2^{R323Q}$) and β3 subunit ($\beta3^{Y302C}$), and the M1 region ($\beta3^{S254F}$). The $\beta3^{D120}$ and $\beta3^{Y302}$ residues are located at the interface of the α1 and β3 subunits, the $\beta3^{T157M}$ residue is located within the β-sheet of the β3 subunits, and the $\beta3^{S254}$ residue is located at the interface of a β3 and α1 subunit or at the interface of a β3 and γ2 subunit.

For the γ2 mutation, we introduced a single copy of the $\gamma2^{R323Q}$ mutation into the first subunit of the concatenated construct. For each of the β3 mutations, we created a set of three constructs with a mutation in either the second or fourth β3 subunit and a construct with a mutation in both the second and fourth β3 subunits (Fig. 3*A*). We injected 2 ng of cRNA encoding for each of the constructs and then compared the absolute currents elicited by 3 mM GABA at the mutant receptors with the WT (Fig. 3*B*).

Strikingly, the incorporation of two mutations into the receptor was catastrophic for three of the β3 mutations. When two copies of the $\beta3^{D120N}$ or $\beta3^{T157M}$ mutations were incorporated into the concatemer, the GABA-elicited currents were too small to be measured, whereas the incorporation of two $\beta3^{Y302C}$ mutations significantly reduced the GABA-elicited currents ($I_{3\ mM\_GABA}$ = 77 nA, γ2-$\beta3^{Y302C}$-α1-$\beta3^{Y302C}$-α1; $I_{3\ mM\_GABA}$ = 2.1 μA, WT). In contrast, there was no significant difference in the current amplitudes compared with WT when two copies of the $\beta3^{S254F}$ mutation were incorporated into the receptor ($I_{3\ mM\_GABA}$ = 1.5 μA, γ2-$\beta3^{S254F}$-α1-$\beta3^{S254F}$-α1) (Fig. 3, *B* and *C*).

In contrast, the incorporation of a single mutation into the receptor did not cause the same marked effects on the magnitude of absolute currents, with no more than a 3-fold reduction at any mutated concatemer. A single $\gamma2^{R323Q}$ mutation in the first subunit of the concatemer had similar GABA-activated currents ($I_{3\ mM\_GABA}$ = 1.4 μA, $\gamma2^{R323Q}$-β3-α1-β3-α1) to WT, whereas the introduction of a single $\beta3^{D120N}$ mutation at either subunit location significantly reduced current amplitudes ($I_{3\ mM\_GABA}$ = 700 and 970 nA, γ2-$\beta3^{D120N}$-α1-β3-α1 and γ2-β3-α1-$\beta3^{D120N}$-α1, respectively). When introduced at the first β3 subunit, a single $\beta3^{T157M}$ or $\beta3^{S254F}$ mutation significantly reduced the current amplitudes ($I_{3\ mM\_GABA}$ = 1.1 and 1.2 μA, γ2-$\beta3^{T157M}$-α1-β3-α1 and γ2-$\beta3^{S254F}$-α1-β3-α1, respectively), but not when introduced in the second ($I_{3\ mM\_GABA}$ = 2.0 and 2.5 μA, γ2-β3-α1-$\beta3^{T157M}$-α1 and γ2-β3-α1-$\beta3^{S254F}$-α1 concatemers, respectively). A single $\beta3^{Y302C}$ mutation significantly reduced GABA-activated currents when introduced in the second β3 subunit, but not the first ($I_{3\ mM\_GABA}$ = 1.3 and 1.8 μA, γ2-β3-α1-$\beta3^{Y302C}$-α1 and γ2-$\beta3^{Y302C}$-α1-β3-α1, respectively) (Fig. 3, *B* and *C*).

Although several concatemers containing single mutations had significant reductions in the maximum absolute currents elicited by 3 mM GABA, this crude approach is a poor measure of how mutations alter receptor properties. Variation in the maximum absolute current can be introduced in several ways

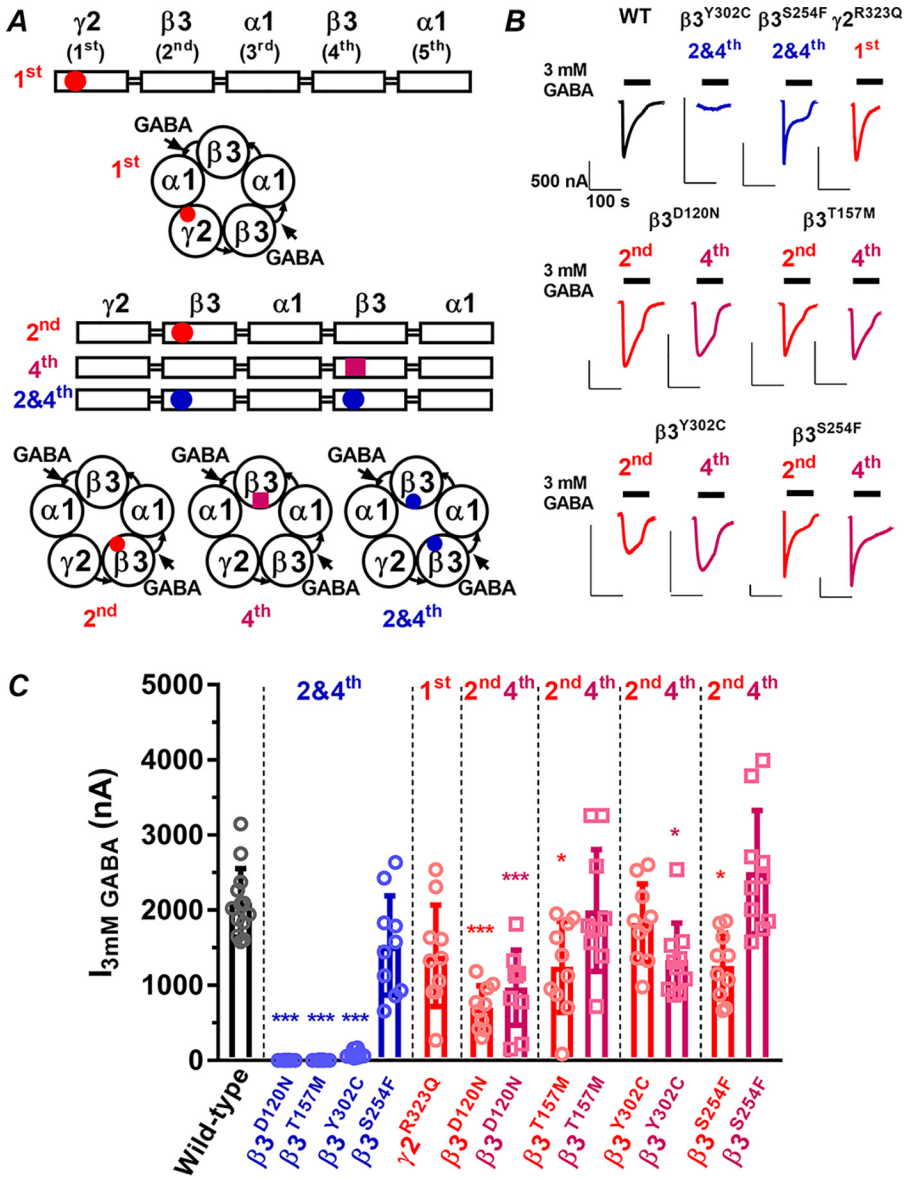

Figure 3. *A*, *schematic* of concatenated receptor indicating the location of mutations when they are introduced into the γ2 or distinct β3 subunits. *Red circles* indicate the location of mutations on the first γ2 subunit, and *red circles*, *purple squares*, and *blue circles* indicate location of mutations on the second, fourth, or both second and fourth β3 subunits, respectively. *B*, representative traces of WT and $\gamma2^{R323Q}$, $\beta3^{D120N}$, $\beta3^{T157M}$, $\beta3^{S254F}$, and $\beta3^{Y302C}$ mutant receptors with mutation(s) in the labeled locations after application of reference 3 mM GABA (*filled bars*). *Scale bars*, 500 nA and 100 s. *C*, absolute current elicited by 3 mM GABA after injection of 2 ng of RNA. Individual data points are depicted as either *open circles* or *squares* with WT as *black bars* and *gray circles* and a *color* and *pattern scheme* identical to that in *A*. *Bars* and *error bars* represent mean ± S.D. of 10–13 individual cells. *, $p < 0.05$; **, $p < 0.01$; ***, $p < 0.001$ compared with WT, one-way ANOVA with Tukey's post hoc test.

that are a consequence of experimental conditions. These include large rightward shifts in the EC_{50} and small changes in the RNA concentration, the incubation time, and the rate at which the individual oocytes form protein and express receptors at the cell surface. However, mutations may also cause changes in the intrinsic activation properties of the receptor that reduce the current passing across the synapse. This can occur through changes in the potency of GABA or changes in the efficacy, where GABA reverts to a more partial agonist, or both. To determine whether the mutations changed either the potency or efficacy of GABA activation, we next constructed concentration–response curves to GABA and estimated the maximum open probability of GABA to determine whether the mutations changed these intrinsic activation properties of the receptor, when either one or two copies of the mutation were present.

$\gamma2^{R323Q}$ impairs GABA activation properties of the receptor

We therefore constructed concentration–response curves to GABA and standardized the response against an estimated maximum open probability of the receptor for the WT and each mutation. We initially compared the $\gamma2^{R323Q}$-β3-α1-β3-α1 mutant receptor with the WT, as this mutation is incorporated into the receptor within the only γ2 subunit (Fig. 4*A*). The potency of GABA has previously been shown to be reduced at α1β2γ2 receptors when expressed in HEK293 cells, and we would expect comparable results in our concatenated construct (15).

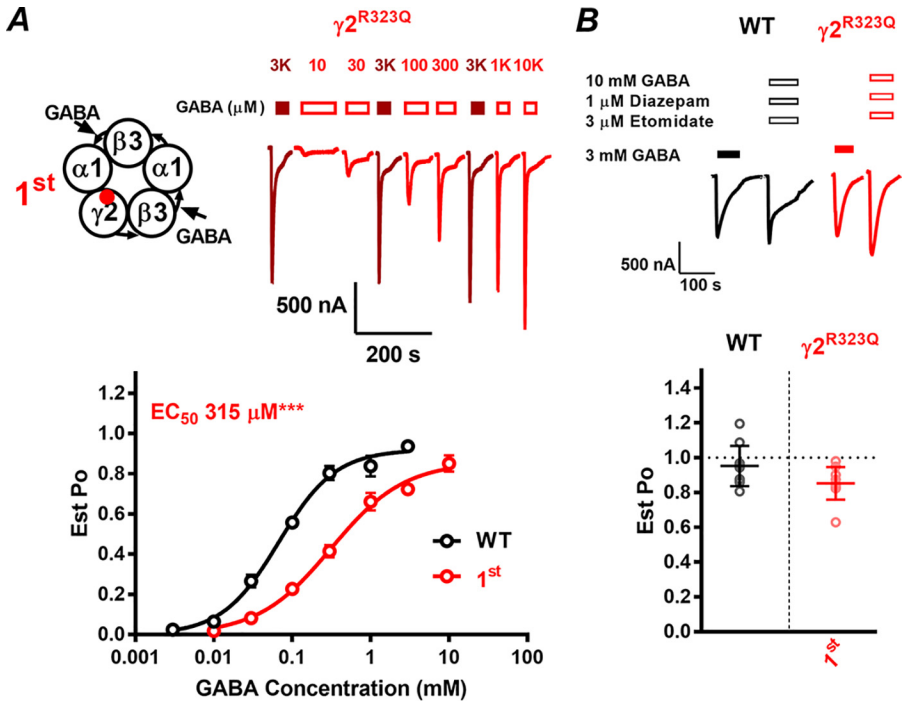

Figure 4. *A*, *schematic* of concatenated receptor indicating the location of the $\gamma2^{R323Q}$ mutation (*red circle*) within the concatenated construct (*left*). Shown are representative data (*right*) from a single two-electrode voltage clamp experiment where different concentrations of GABA (*open bars*) were applied to construct a concentration–response curve to GABA at $\gamma2^{R323Q}$-$\beta3$-$\alpha1$-$\beta3$-$\alpha1$ receptors. *Filled dark red bars* and *traces* represent reference 3 mM GABA applications, and *open red bars* and *traces* represent GABA applications at the concentrations shown. Shown is a concentration–response curve to GABA (*below*) of WT $\gamma2$-$\beta3$-$\alpha1$-$\beta3$-$\alpha1$ (○) and $\gamma2^{R323Q}$-$\beta3$-$\alpha1$-$\beta3$-$\alpha1$ (○) receptors normalized to the Est. $P_{o(max)}$ and fitted to the Hill equation. *Dots*, mean ± S.E. (*error bars*) of 10–13 individual experiments. The EC_{50} of the mutant receptor derived from the curve fit is shown. *, $p < 0.05$; **, $p < 0.01$; ***, $p < 0.001$ compared with WT, one-way ANOVA with Tukey's post hoc test. *B*, representative traces of WT (*black*) and $\gamma2^{R323Q}$ (*red*) mutant receptors after application of reference 3 mM GABA (*filled bars*) and 10 mM GABA, 1 μM diazepam, and 3 μM etomidate (*open bars*), respectively. *Scale bars*, 500 nA and 100 s. The Est. GABA $P_{o(max)}$ of WT (○) and $\gamma2^{R323Q}$ (○) mutant receptors (*below*) was determined by dividing the current elicited by 3 mM GABA by the current elicited by 10 mM GABA, 1 μM diazepam, and 3 μM etomidate and corrected for the reference 3 mM GABA current. *Lines* and *error bars* represent the mean ± S.D. of 10 individual cells.

We first tested whether the $\gamma2^{R323Q}$ mutation altered the potency of GABA. We constructed concentration–response curves to GABA at $\gamma2^{R323Q}$-$\beta3$-$\alpha1$-$\beta3$-$\alpha1$ receptors to determine the EC_{50} of the mutant receptors. These experiments were run on an automated protocol, where 3 mM GABA was applied as a reference and internal standard three times during the experiment for all receptors (Fig. 4*A*). Similar to the results reported using this mutation with free $\alpha1$ and $\beta3$ subunits in HEK293 cells (15), there was a decrease in the potency of GABA with a significant 4.5-fold decrease in the potency of GABA (EC_{50} = 315 μM) (Fig. 4*A* and Table 1), demonstrating that the activation of receptors by GABA is impaired by the $\gamma2^{R323Q}$ mutation.

We then determined whether the maximal efficacy of GABA was impaired by the $\gamma2^{R323Q}$ mutation by estimating the maximum P_o (Est. $P_{o(max)}$) at WT and $\gamma2^{R323Q}$-$\beta3$-$\alpha1$-$\beta3$-$\alpha1$ receptors using a pharmacological technique similar to Shin *et al.* (30). At oocytes expressing either WT or mutant receptors, we applied the 3 mM GABA reference and then co-applied 10 mM GABA with 1 μM etomidate and 3 μM diazepam to shift as many receptors as possible to the open state (Fig. 4*B*). We assumed that the combination of GABA with etomidate and diazepam opened the receptors with a probability approaching 1. The Est. $P_{o(max)}$ of GABA for each receptor was then calculated by dividing the current elicited by 3 mM GABA by the current elicited by GABA, etomidate, and diazepam and corrected to account for shifts in the concentration–response curves (Fig. 4*B* and Table 1). We refer to Est. $P_{o(max)}$ as an *estimated* maximum open probability as the true current amplitude may be underestimated by mutations that greatly impair receptor activation or modulation or change desensitization kinetics. As expected, GABA elicited a very high Est. $P_{o(max)}$ of 0.95 at WT receptors, consistent with single-channel recordings where the channel enters a long-lived open state (31). The $\gamma2^{R323Q}$ mutation did not significantly alter the Est. $P_{o(max)}$ with a value of 0.85 (Fig. 4*B* and Table 1).

When incorporated into the first subunit of the concatemer, the $\gamma2^{R323Q}$ mutation reduced the potency of GABA without causing a significant reduction in the efficacy. These changes in the activation properties of the receptor caused by the $\gamma2^{R323Q}$ mutation in the concatenated construct were similar to the reported effects of receptors composed of unlinked subunits. Therefore, the concatenated construct is a suitable method of analyzing the effect of mutations on the activation properties of the receptor.

A single $\beta3^{D120N}$ or $\beta3^{T157M}$ mutation impairs GABA potency, and two mutations are catastrophic

We next assessed the effects of two $\beta3$ mutations, $\beta3^{D120N}$ and $\beta3^{T157M}$, that are both located in the extracellular domain at the earlier stages of the activation pathway. The $\beta3^{D120N}$ mutation has previously been expressed in combination with either $\alpha1$, $\beta3$, and $\gamma2$ or $\alpha1$ and $\gamma2$ free subunits to determine the effects of heterozygous or homozygous expression, respec-

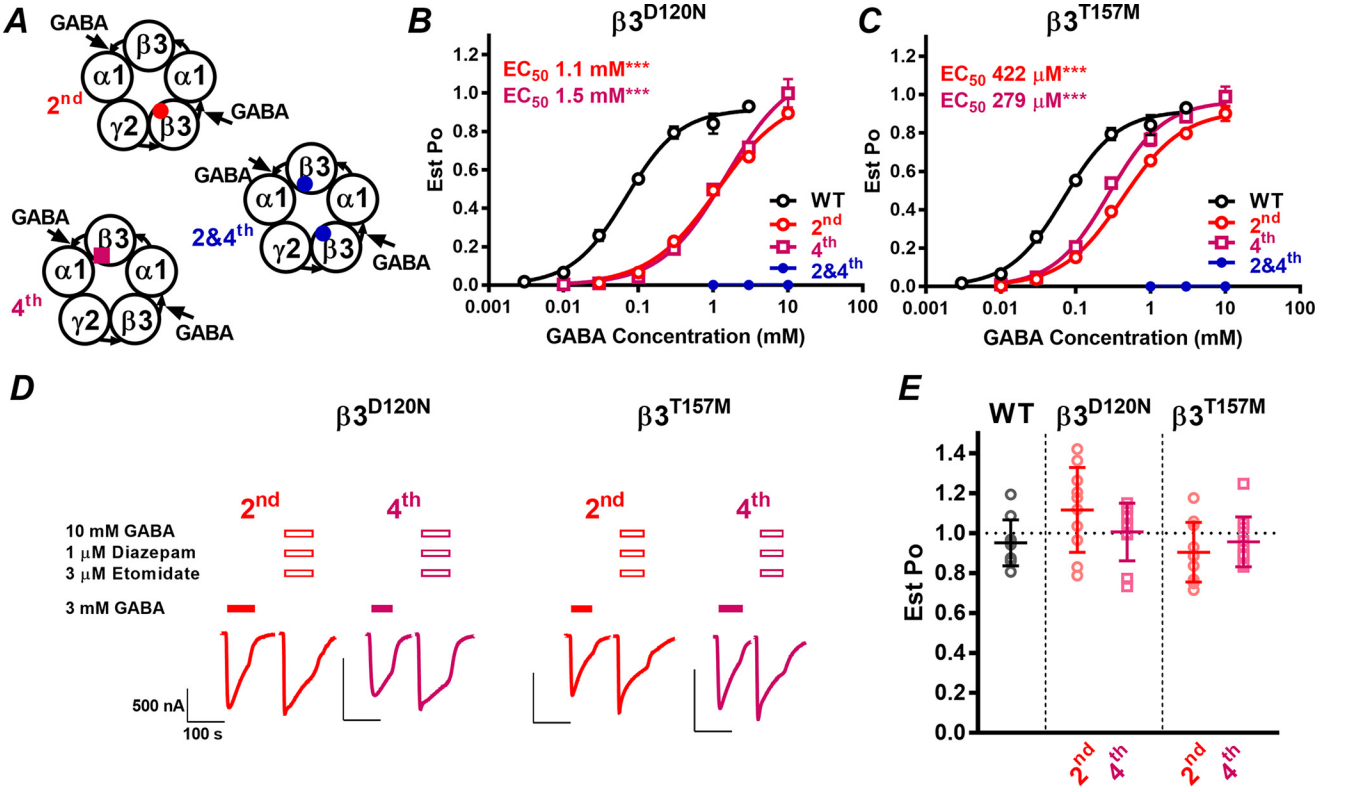

Figure 5. *A, schematic* of concatenated receptor indicating the location of $\beta3^{D120N}$ and $\beta3^{T157M}$ mutations introduced within the second (*closed red circle*), fourth (*closed purple square*) or the second and fourth (*closed blue circles*) subunits within the resulting pentameric receptor. *B*, concentration–response curve to GABA of WT $\gamma2$-$\beta3$-$\alpha1$-$\beta3$-$\alpha1$ (*open black circle*), $\gamma2$-$\beta3^{D120N}$-$\alpha1$-$\beta3$-$\alpha1$ (*open red circle*), $\gamma2$-$\beta3$-$\alpha1$-$\beta3^{D120N}$-$\alpha1$ (*open purple square*), and $\gamma2$-$\beta3^{D120N}$-$\alpha1$-$\beta3^{D120N}$-$\alpha1$ (*closed blue circle*) receptors; *C*, Concentration–response curve to GABA of WT $\gamma2$-$\beta3$-$\alpha1$-$\beta3$-$\alpha1$ (*open black circle*), $\gamma2$-$\beta3^{T157M}$-$\alpha1$-$\beta3$-$\alpha1$ (*open red circle*), $\gamma2$-$\beta3$-$\alpha1$-$\beta3^{T157M}$-$\alpha1$ (*open purple square*), and $\gamma2$-$\beta3^{T157M}$-$\alpha1$-$\beta3^{T157M}$-$\alpha1$ (*closed blue circle*) receptors normalized to the Est. $P_{o(max)}$ and fitted to the Hill equation. The EC_{50} of the mutant receptor derived from the curve fit is shown. *, $p < 0.05$; **, $p < 0.01$; ***, $p < 0.001$ compared with WT, one-way ANOVA with Tukey's post hoc test. *D*, representative traces of $\beta3^{D120N}$ and $\beta3^{T157M}$ receptors after application of 3 mM GABA (*filled bars*) and 10 mM GABA, 1 μM diazepam, and 3 μM etomidate (*open bars*), respectively. *Red traces* indicate mutation at the second subunit location, and *purple traces* indicate mutation at the fourth. *Scale bars*, 500 nA and 100 s. *E*, estimated GABA $P_{o(max)}$ of WT, $\beta3^{D120N}$, and $\beta3^{T157M}$ receptors was determined by dividing the current elicited by 3 mM GABA by the current elicited by 10 mM GABA, 1 μM diazepam, and 3 μM etomidate and corrected for the reference 3 mM GABA. *Open gray circles*, WT; *open red circles*, receptors with a mutation in the second position; *open purple squares*, receptors with a mutation in the fourth position. *Lines* and *error bars* represent mean ± S.D. of 10 individual cells.

tively, on receptor function (11). Both the gating properties and the absolute expression levels of the receptor were reduced in both cases, whereas in a separate study, the incorporation of the $\beta3^{T157M}$ mutation with $\alpha5$ and $\gamma2$ subunits only made subtle changes to the activation properties of the receptor (8). To determine the effect of the mutations when they were expressed in a single subunit within the receptor, we constructed concentration–response curves to GABA and measured the Est. $P_{o(max)}$ at concatenated receptors containing a single copy of a mutation.

We created concatenated constructs by introducing $\beta3^{D120N}$ or $\beta3^{T157M}$ mutations in the second, the fourth or both the second and fourth subunits in the concatemer and constructed concentration–response curves to GABA (Fig. 5*A*). A single copy of the $\beta3^{D120N}$ mutation significantly reduced the potency of GABA by 16–20-fold, regardless of whether it was introduced at the second or fourth subunit (EC_{50} = 1.14 and 1.47 mM, $\gamma2$-$\beta3^{D120N}$-$\alpha1$-$\beta3$-$\alpha1$ and $\gamma2$-$\beta3$-$\alpha1$-$\beta3^{D120N}$-$\alpha1$, respectively) (Fig. 5*B* and Table 1). These EC_{50} values were not significantly different from each other, strongly suggesting that the subunit location of the $\beta3^{D120N}$ mutation within the pentameric structure did not affect how the mutation altered receptor activation properties.

Similarly, the $\beta3^{T157M}$ mutations significantly reduced the potency of GABA by 4–6-fold when introduced at either the second or fourth subunit (EC_{50} = 422 and 279 μM, $\gamma2$-$\beta3^{T157M}$-$\alpha1$-$\beta3$-$\alpha1$ and $\gamma2$-$\beta3$-$\alpha1$-$\beta3^{T157M}$-$\alpha1$, respectively) (Fig. 5*C* and Table 1). Again, the EC_{50} values were not significantly different from each other, demonstrating that the subunit location of the $\beta3^{T157M}$ did not affect how the mutation altered the activation properties of GABA. Neither receptor expressed measurable currents when a mutation was introduced in both $\beta3$ subunits, and as such, concentration–response curves could not be constructed.

We next measured the Est. $P_{o(max)}$ of two receptors with a single copy of the mutation in the second or fourth subunit, respectively, to determine whether the efficacy of GABA had been altered (Fig. 5*D*). Despite the absolute current levels being reduced by the $\beta3^{D120N}$ mutation, the combination of etomidate and diazepam failed to appreciably increase the maximal response to GABA at either receptor containing a single mutation (Fig. 5, *D* and *E*). This is likely due in part to the large rightward shift of the concentration–response curve where 3 mM GABA no longer elicits the maximum response. Similarly, the combination of etomidate and diazepam had little effect on the maximal GABA current elicited at the two receptors containing a single $\beta3^{T157M}$ mutation (Fig. 5, *D* and *E*). Consequently, there was no significant difference in the Est. $P_{o(max)}$ at the four receptors (Est. $P_{o(max)}$ = 1.12, 1.00, 0.9, and 0.96,

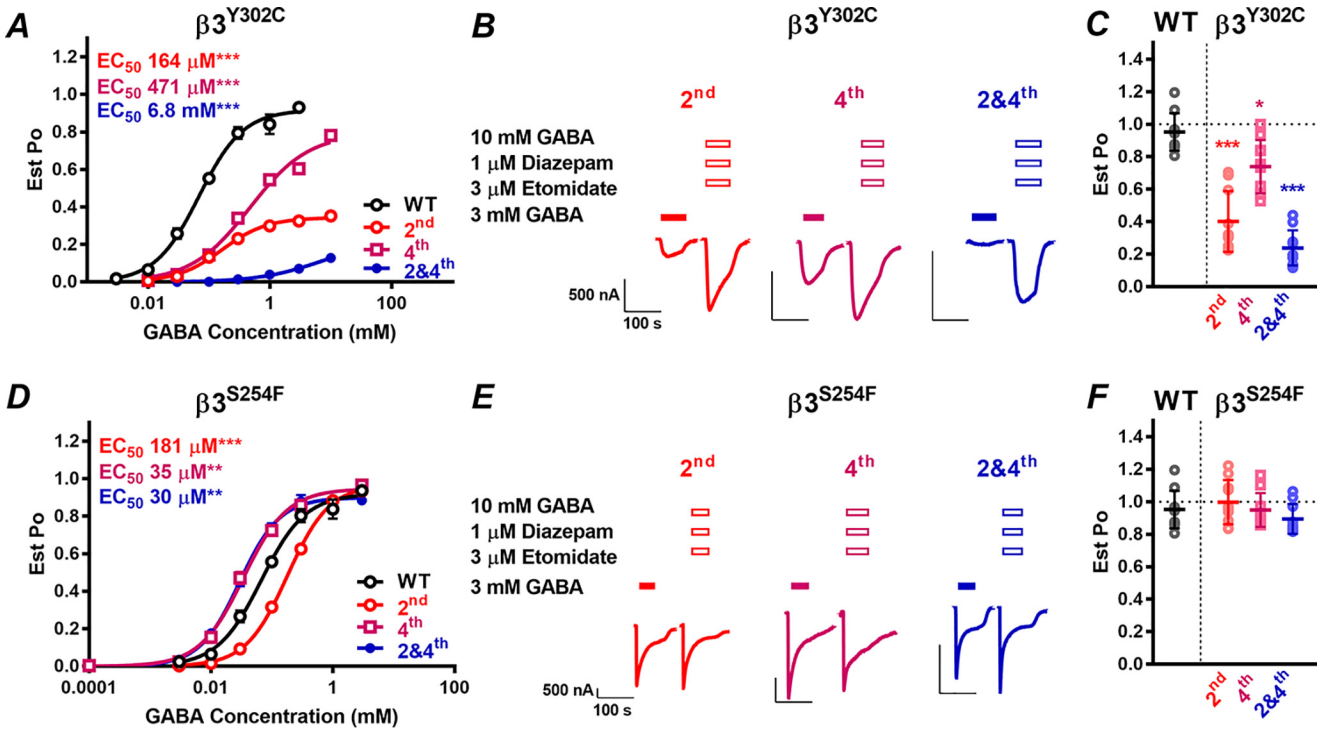

Figure 6. *A*, concentration–response curve to GABA of WT γ2-β3-α1-β3-α1 (*open black circles*), γ2-β3^{Y302C}-α1-β3-α1 (*open red circles*), γ2-β3-α1-β3^{Y302C}-α1 (*open purple squares*) and γ2-β3^{Y302C}-α1-β3^{Y302C}-α1 (*closed blue circles*) receptors normalized to the Est. $P_{o(max)}$ and fitted to the Hill equation. *Dots*, mean ± S.E. (*error bars*) of 10–13 individual experiments. The EC_{50} of the mutant receptor derived from the curve fit is shown. *, $p < 0.05$; **, $p < 0.01$; ***, $p < 0.001$ compared with WT, one-way ANOVA with Tukey's post hoc test. *B*, representative traces of β3^{Y302C} mutant receptors after application of reference 3 mM GABA (*filled bars*) and 10 mM GABA, 1 μM diazepam, and 3 μM etomidate (*open bars*), respectively. *Red traces* indicate mutation at the second subunit location, *purple* indicates mutation at the fourth subunit location, and *blue* indicates mutation at both the second and fourth locations. *Scale bars*, 500 nA and 100 s. *C*, estimated GABA $P_{o(max)}$ of WT γ2-β3-α1-β3-α1 (*open black circles*), γ2-β3^{Y302C}-α1-β3-α1 (*open red circles*), γ2-β3-α1-β3^{Y302C}-α1 (*open purple squares*) and γ2-β3^{Y302C}-α1-β3^{Y302C}-α1 (*closed blue circles*) mutant receptors. Est. $P_{o(max)}$ was determined by dividing the current elicited by 3 mM GABA by the current elicited by 10 mM GABA, 1 μM diazepam, and 3 μM etomidate and corrected where 3 mM GABA was not at the maximum of the concentration–response curves. *Lines* and *bars*, mean ± S.D. of 10 individual cells. *, $p < 0.05$; **, $p < 0.01$; ***, $p < 0.001$ compared with WT, one-way ANOVA with Tukey's post hoc test. *D*, concentration–response curve to GABA of WT γ2-β3-α1-β3-α1 (*open black circles*), γ2-β3^{S254F}-α1-β3-α1 (*open red circles*), γ2-β3-α1-β3^{S254F}-α1 (*open purple squares*), and γ2-β3^{S254F}-α1-β3^{S254F}-α1 (*closed blue circles*) receptors normalized to the Est. $P_{o(max)}$ and fitted to the Hill equation. *Dots*, mean ± S.E. of 10–13 individual experiments. The EC_{50} of the mutant receptor derived from the curve fit is shown. *, $p < 0.05$; **, $p < 0.01$; ***, $p < 0.001$ compared with WT, one-way ANOVA with Tukey's post hoc test. *E*, representative traces of β3^{Y302C} mutant receptors after application of reference 3 mM GABA (*filled bars*) and 10 mM GABA, 1 μM diazepam, and 3 μM etomidate (*open bars*), respectively. *Red traces*, mutation at the second subunit location; *purple traces*, mutation at the fourth subunit location; *blue traces*, mutation at both the second and fourth locations. *Scale bars*, 500 nA and 100 s. *F*, estimated GABA $P_{o(max)}$ of WT γ2-β3-α1-β3-α1 (*open gray circles*), γ2-β3^{S254F}-α1-β3-α1 (*open red circles*), γ2-β3-α1-β3^{S254F}-α1 (*open purple squares*), and γ2-β3^{S254F}-α1-β3^{S254F}-α1 (*closed blue circles*) mutant receptors. Est. $P_{o(max)}$ was determined by dividing the current elicited by 3 mM GABA by the current elicited by 10 mM GABA, 1 μM diazepam, and 3 μM etomidate and corrected where 3 mM GABA was not at the maximum of the concentration–response curves. *Lines* and *error bars*, mean ± S.D. of 10 individual cells. *, $p < 0.05$; **, $p < 0.01$; ***, $p < 0.001$ compared with WT, one-way ANOVA with Tukey's post hoc test.

γ2-β3^{D120N}-α1-β3-α1, γ2-β3-α1-β3^{D120N}-α1, γ2-β3^{T157M}-α1-β3-α1, and γ2-β3-α1-β3^{T157M}-α1, respectively) (Fig. 5*E* and Table 1).

Taken together, single copies of the β3^{D120N} and β3^{T157M} mutations at the earlier stages of the activation pathway both impair GABA activation of the receptor by reducing the potency of GABA by ~20- and 5-fold, respectively, without altering the maximal efficacy of GABA. There was little difference in the effect of either single mutation when located at different subunits β3 within a pentamer. A second copy of the β3^{D120N} or β3^{T157M} mutation intensifies the effect of the mutation and appears to be catastrophic, leading to little to no functional receptor expression.

β3^{S254F} and β3^{Y302C} mutation effects are dependent on location and number of mutations

We next assessed the effects of two other β3 mutations, β3^{Y302C} and β3^{S254F}. The β3^{Y302} residue is located in the M2-M3 coupling loop, a key motif in the activation pathway that links extracellular and transmembrane domains. The β3^{S254} residue is located in the transmembrane regions within the M1 transmembrane helix that moves late in the activation process of ligand-gated ion channels (32). The β3^{Y302C} mutation has been shown to impair receptor activation when expressed with either α1 and γ2 subunits or α5 and γ2 receptors (8, 11), whereas there are no functional data on how the β3^{S254F} mutation affects receptor activation.

A single copy of the β3^{Y302C} mutation, introduced at either the second or the fourth subunit, significantly reduced the potency of GABA between 2- and 7-fold (EC_{50} = 167 and 471 μM, γ2-β3^{Y302C}-α1-β3-α1 and γ2-β3-α1-β3^{Y302C}-α1, respectively), and these EC_{50} values differed significantly from each other (Fig. 6*A* and Table 1). Two copies of the β3^{Y302C} mutation were catastrophic, further reducing the potency of GABA by nearly 100-fold, an order of magnitude greater than either of the single mutations (EC_{50} = 6.81 mM, γ2-β3^{Y302C}-α1-β3^{Y302C}-α1). This EC_{50} value was significantly greater than the

EC_{50} value of the WT or the two concatemers containing a single $\beta3^{Y302C}$ mutation (Fig. 6*A* and Table 1).

Additionally, the introduction of the $\beta3^{Y302C}$ mutation significantly reduced the Est. $P_{o(max)}$ compared with WT, regardless of the subunit location of the mutation or whether one or two copies of the mutation were introduced. The efficacy of GABA was least affected by one copy of the $\beta3^{Y302C}$ mutation at the fourth subunit (Est. $P_{o(max)} = 0.74$, $\gamma2$-$\beta3$-$\alpha1$-$\beta3^{Y302C}$-$\alpha1$), whereas a single copy of the $\beta3^{Y302C}$ mutation at the second subunit significantly reduced the efficacy of GABA compared with the WT or the receptor with a single mutation at the fourth subunit (Est. $P_{o(max)} = 0.4$, $\gamma2$-$\beta3^{Y302C}$-$\alpha1$-$\beta3$-$\alpha1$). Two copies of the $\beta3^{Y302C}$ mutation resulted in the lowest efficacy of GABA ($P_{o(max)} = 0.24$, $\gamma2$-$\beta3^{Y302C}$-$\alpha1$-$\beta3^{Y302C}$-$\alpha1$) (Fig. 6 (*B* and *C*) and Table 1). This demonstrates that, unique among the mutations that we have investigated, the single $\beta3^{Y302C}$ mutation impairs activation of the receptor to decrease both the potency and maximum efficacy of GABA activation. Differences in the magnitude of the reduction in the maximal efficacy suggest that these residues may not be equivalent when located in different subunits.

The introduction of the $\beta3^{S254F}$ mutation did not follow the same pattern as the other mutations, which reduced the potency of GABA regardless of the subunit location of the mutation. Instead, when the mutation was introduced at the second subunit, the EC_{50} value of GABA was significantly increased nearly 3-fold compared with the WT ($EC_{50} = 181$ μM, $\gamma2$-$\beta3^{S254F}$-$\alpha1$-$\beta3$-$\alpha1$), demonstrating that the activation properties of this concatemer were impaired (Fig. 6*D* and Table 1). However, when the mutation was introduced at the fourth subunit, the EC_{50} value of GABA significantly decreased 2-fold compared with the WT, as did the EC_{50} when the $\beta3^{S254F}$ mutation was introduced at both the second and fourth subunits ($EC_{50} = 34.2$ and 29.6 μM, $\gamma2$-$\beta3$-$\alpha1$-$\beta3^{S254F}$-$\alpha1$ and $\gamma2$-$\beta3^{S254F}$-$\alpha1$-$\beta3^{S254F}$-$\alpha1$, respectively) (Fig. 6*D* and Table 1). This demonstrates that the subunit location of the $\beta3^{S254F}$ mutation defines the functional effect of the receptor, determining whether the potency of GABA has increased or decreased.

The maximal efficacy of GABA was not changed by the $\beta3^{S254F}$, regardless of whether one or two copies of the mutation were incorporated into the concatemer (Est. $P_{o(max)} =$ 1.00, 0.95, and 0.89, $\gamma2$-$\beta3^{S254F}$-$\alpha1$-$\beta3$-$\alpha1$, $\gamma2$-$\beta3$-$\alpha1$-$\beta3^{S254F}$-$\alpha1$, and $\gamma2$-$\beta3^{S254F}$-$\alpha1$-$\beta3^{S254F}$-$\alpha1$, respectively) (Fig. 6 (*E* and *F*) and Table 1). The differences in the EC_{50} value at receptors with a single $\beta3^{S254F}$ mutation at different subunit locations suggest that these locations are not equivalent in the activation pathway.

Discussion

Recent advances in whole-genome sequencing have enabled the identification of a large number of *de novo* mutations that cause a range of severe childhood epilepsies. In all of these cases, the mutations are dominant (2–16), whereby patients will contain one WT and one mutant copy of the gene. In cases where the mutations are in the $\beta3$ subunit of the GABA$_A$ receptor, this will lead to several potential receptors being expressed in each subtype, with heteromutant receptors containing single mutations at either of the two $\beta3$ subunits and a homomutant receptor containing mutations at both $\beta3$ subunits. Precise functional genomic analysis requires the understanding of how each of these individual receptors are affected by the mutation, as these receptors could be expressed and contribute to the pathology of the disorder or even be targeted by GABAergic drugs to treat the seizures.

The *in vitro* analysis of these mutations has, to date, relied solely on injection or transfection of WT and/or mutant subunits in heterologous systems and quantification of receptor expression levels complemented with whole-cell recording and, at times, single-channel analysis (8, 11, 15). However, this approach is inadequate to describe the entire molecular phenotype, as mixed populations of receptors with one or two mutations will form at a ratio of 2:1. This will be particularly problematic when the maximal efficacy is reduced by the mutation, as the higher efficacy of the WT receptor will dominate the signal in whole-cell recordings. Therefore, by using a concatenated receptor construct, we have derived results from heteromutant $\beta3$ receptors that provide significant insights into the molecular phenotypes of epilepsies caused by GABA$_A$ receptor mutations as well as knowledge about the activation mechanisms of these receptors.

Mutations impair synaptic transmission through efficacy or potency of GABA activation

There is an enormous amount of understanding of how GABA$_A$R opening is triggered through an activation pathway initiated by GABA binding that then opens the intrinsic ion channel to mediate neuronal inhibition (22). Briefly, the agonist binds at the interface between a $\beta3$ and an $\alpha1$ subunit at the extracellular domain, causing a series of conformational changes within the receptor that lead to the transmembrane domains. At the interface of the extracellular and transmembrane domains, a set of interacting loops, including the $\beta1$-$\beta2$, $\beta6$-$\beta7$, and $\beta8$-$\beta9$ in the extracellular domain and pre-M1 and M2-M3 loops connecting the transmembrane domain, alter their conformation during receptor activation (33, 34). This leads to a tilting of the M2 helices and ultimately channel opening. Additionally, the number of molecules bound is important, where two molecules of agonist are required to be bound to fully activate the receptor (35).

Synaptic receptors that contain a $\gamma2$ subunit typically have intrinsic activation properties distinct from those of extrasynaptic receptors that contain a δ subunit, including a high efficacy where the maximal open probability elicited by GABA approaches 1 and lower potency (31, 36). The maximal efficacy of an agonist, or whether the agonist is partial or full, is largely defined by transitional conformational states, known as preactivated or "flip" states, that precede the final conformational change that opens the channel gate (37). Residues at the earlier stage of the activation pathway (11) appear to have no influence on the maximal efficacy of GABA, with $\beta3^{D120N}$ and $\beta3^{T157M}$ single mutations having an efficacy similar to that of WT. At these mutations, located near the ligand-binding domain and within an extracellular structural β-sheet, respectively, GABA remains acting as essentially a "full" agonist, activating the receptor with a very high maximal open probability.

However, the $\beta3^{Y302C}$ mutations in the M2-M3 loop change the intrinsic property of receptor activation such that the max-

imal efficacy of GABA is significantly reduced. Essentially, GABA has become a "partial" agonist at these receptors, where the mutation in the coupling region may be destabilizing transitional conformational states. Further, the efficacy of GABA was different, depending on the subunit location of the $\beta3^{Y302C}$ mutation, suggesting that the two mutations are not entirely equivalent.

Asymmetrical effects of the same mutation at different subunit locations

A notable feature of these mutations is the differential effect of the $\beta3^{S254F}$ mutation when located at different subunit locations and slightly different levels of reductions in the efficacy of GABA at receptors with a $\beta3^{Y302C}$ mutation in different locations. This is in contrast with the $\beta3^{D120N}$ and $\beta3^{T157M}$ mutations, where the location of the individual mutations had no significant effect. It is known that the pseudosymmetry of the pentameric receptor can cause positional effects of mutations (38), and there are two possible reasons for these differences. First, the local environment surrounding mutated residues may be identical at the two subunit locations for some mutations but not others. Second, the conformational changes during the activation process may not be symmetrical from ligand binding to channel opening. Furthermore, in epilepsy-causing mutations that impair surface expression, the location of the mutation can also determine the severity of the effect (39).

Recent advances in cryogenic EM (cryo-EM) have enabled the solving of many membrane-bound proteins to a very fine resolution. During the preparation of this manuscript, a cryo-EM structure of the $\alpha1\beta3\gamma2$ receptor with and without GABA and diazepam bound and a structure of the $\alpha1\beta1\gamma2$ receptor were published (40, 41). The sequences between the $\beta2$ and $\beta3$ subunits are highly homologous and identical within the regions containing the mutations studied. Hence, we can utilize the cryo-EM structure to explain the positional effects, or lack thereof, of our mutations.

Within the GABA and diazepam-bound $\alpha1\beta3\gamma2$ structure, the $\beta3^{120}$ residue was located within the general vicinity of the ligand-binding site at the interface of the $\beta3$ and $\alpha1$ subunits (Fig. 7*A*) (11, 41). The cryo-EM structure indicated that the local environment surrounding the $\beta3^{120}$ residues is identical, making contacts with the adjacent $\alpha1^{M141}$ and $\alpha1^{P142}$ residues regardless of the subunit the mutation is in (Fig. 7*A*). Similarly, the $\beta3^{T157}$ residue is located within a β-sheet within the interior of the $\beta3$ subunit, where the amino acid side chains interact entirely with residues within the $\beta3$ subunit, and the local environment that surrounds the amino acid residues is identical (Fig. 7*B*). Therefore, the similarity of the functional changes caused by mutations at these residues suggests that both of the local environments are identical and that the conformational changes at these initial stages of the activation pathway are symmetrical.

The $\beta3^{Y302}$ residue is located in the M2-M3 loop, a key motif in the coupling of ligand binding to channel gating that moves considerably during the channel activation process. Although there are differences in the activation processes of single $\beta3^{Y302C}$ mutant receptors, depending on the subunit that the mutation is located in, the local environment surrounding the $\beta3^{Y302}$ residue is similar at the two subunits (Fig. 7*C*). There are slightly different poses for the $\beta3^{Y302}$ residue in each of the different locations, but it is known that the M2-M3 region alters conformation during the gating process (42), and it may be differences in the conformational changes that cause subtle differences in the effect of the mutation when it is present at the different locations.

The cryo-EM structure of the $\alpha1\beta1\gamma2$ GABA$_A$ receptor identified asymmetry within the transmembrane regions of the receptor (40). Whereas the distance between subunits was the same, the angles in the pentamer substantially differed along with the tilt of the transmembrane helices when compared with the $\beta3$ subunit. This asymmetry of key secondary structures may contribute to the $\beta3^{Y302C}$ mutation having different effects when introduced in different regions within the transmembrane regions of GABA$_A$ receptors, where the transitional or pre-activated states are subtly different at the coupling regions, depending on where the first GABA molecule is bound.

The $\beta3^{S254F}$ mutation caused markedly different effects, depending on the subunit where the mutation was introduced. The $\beta3^{S254}$ residue is located deep within the transmembrane region of the M1 helix, where it can interact with other transmembrane helices, including the M2 helix of the adjacent subunit.

The M1 helix of one $\beta3$ subunit is adjacent to the M3 of an $\alpha1$ subunit, whereas the M1 helix of the second $\beta3$ subunit is adjacent to the M3 of the $\gamma2$ subunit. This difference may underlie the different functional changes when the mutation is introduced at different locations. The side chains of the $\beta3^{S254}$ residues themselves make intrasubunit interactions within the $\beta3$ subunit, and the introduction of the phenylalanine residue is unlikely to make different side chain interactions when introduced at the two locations (Fig. 8). However, the bulky side chain is likely to cause structural rearrangements when occupying a larger volume, where the backbone of the M1 helix backs onto the M3 helix of either the $\gamma2$ or $\alpha1$ subunit. At a critical part of the M3 helix, the two subunits have different amino acid sequences, and the M3 helices are in markedly different conformations in different cryo-EM structures.

The M3 helix of the $\alpha1$ subunit is parallel to the M1 helix of the $\beta3$ subunit in the apo and GABA and diazepam-bound $\alpha1\beta3\gamma2$ structures (Fig. 8, *A* and *B*). The M3 helix of the $\gamma2$ subunit is similarly parallel in the GABA and diazepam-bound $\alpha1\beta3\gamma2$ structure, but in the apo-structure, the M3 helix of the $\gamma2$ subunit is tilted, angling away from the M1 helix of the $\beta3$ subunit at the extracellular end. Further, the $\gamma2^{F343}$ residue has an altered side-chain conformation. A similar change in the M3 conformation of the M3 helix is also seen in the $\alpha1\beta3\gamma2$ cryo-EM structure (40) (Fig. 8*C*). A plausible reason for the different activation properties of the two single $\beta3^{S254F}$ mutant receptors is that when the residue is mutated adjacent to the $\gamma2$ subunit, the subsequent rearrangements introduce twisting or tilting of the α-helices to favor a closed conformation, but when adjacent to an $\alpha1$ subunit, the interactions stabilize an intermediate or open state.

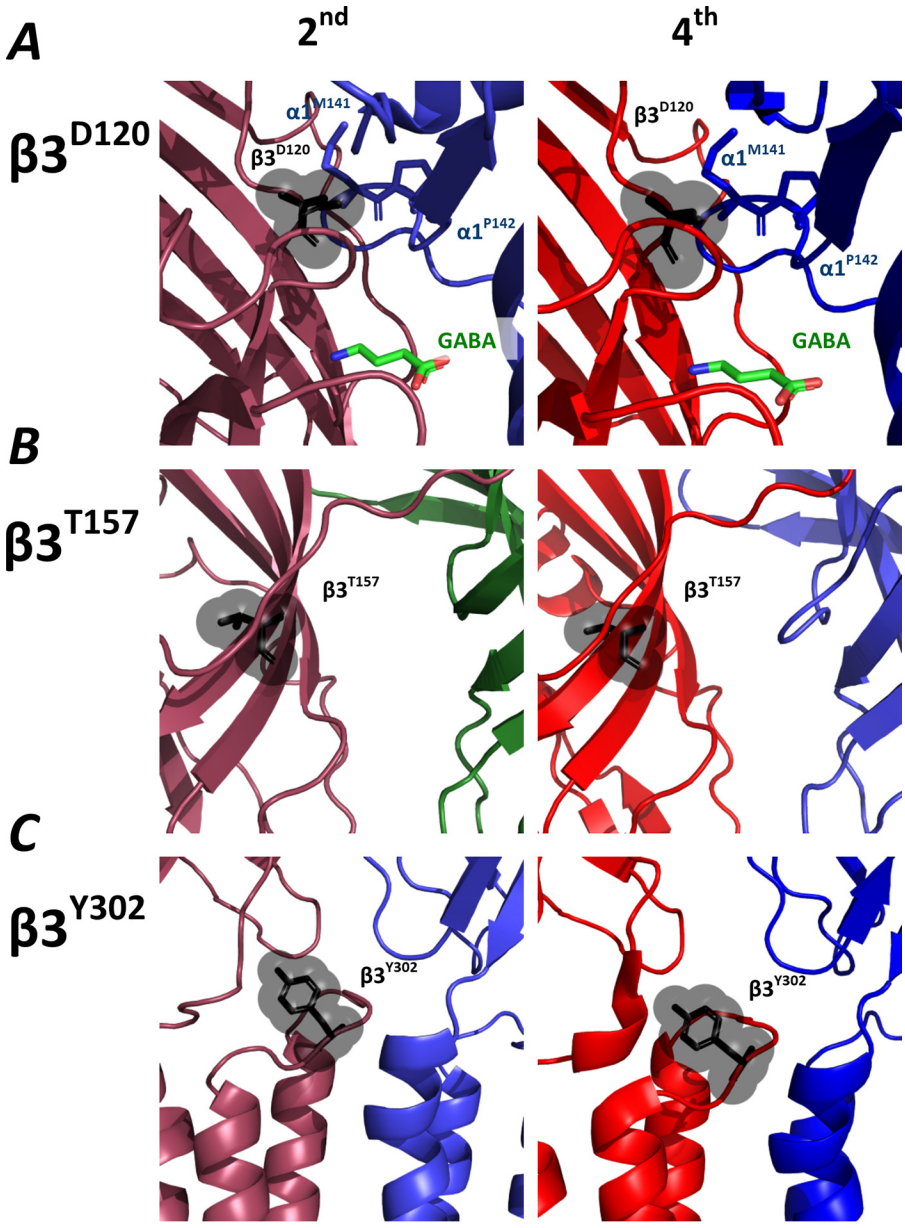

Figure 7. *A–C, enlarged view* of the $\alpha1\beta3\gamma2$ cryo-EM structure (PDB code 6HUP) (41) showing the $\beta3$ mutant residues $\beta3^{D120}$ (*A*), $\beta3^{T157}$ (*B*), and $\beta3^{Y302}$ (*C*) in the two different subunit locations of the second $\beta3$ subunit (*left*) and fourth $\beta3$ subunit (*right*). The subunits are *colored* with the first $\gamma2$ subunit in *green*, the second $\beta3$ subunit in *maroon*, the third $\alpha1$ subunit in *light blue*, the fourth $\beta3$ subunit in *red*, and the fifth $\alpha1$ subunit in *dark blue* and the GABA molecule in *blue*, *red*, and *green*. Residues from the adjacent $\alpha1$ or $\gamma2$ subunits are indicated. At the $\beta1^{D120}$ (*A*), $\beta1^{T1577}$ (*B*), and $\beta1^{Y302}$ (*C*) residues, the interacting partners are identical residues either on the adjacent subunit or within the $\beta3$ subunit itself.

Molecular phenotype of the mutations

There is a wealth of information that suggests that impairment of GABA$_A$ receptor–mediated inhibition can lead to seizures. This includes pharmacological evidence, where antagonists of the GABA$_A$ receptor, such as bicuculline, induce seizures (43), and genetic evidence, where mutations in GABA$_A$ receptor subunits are known to reduce receptor translocation to the cell surface (44) or impair the activation properties of the receptor (8, 11, 13, 15). In this study, we focused on five distinct mutations, four of which clearly impaired the activation by GABA when only a single copy of the mutation was present. Our approach using the concatenated receptor enabled us to assess the complexity of receptors that contain mutations in one or both $\beta3$ subunits.

For three of the mutations, the resulting receptors followed a predictable pattern. A single copy of the mutation, introduced at either $\beta3$ subunit, caused a substantial impairment of the activation of the receptor by GABA. When a second mutation was introduced to the receptor, there was a catastrophic change to the receptor such that the magnitude of currents was either too low to be measured or markedly reduced. Regardless of whether the expression of these receptors is affected by the mutation, we would expect synaptic transmission of GABA-elicited currents to be impaired in the inhibitory pathways within these patients, with receptors containing single mutations mediating reduced neurotransmission and receptors with two copies of the mutation mediating little, if any, chloride current.

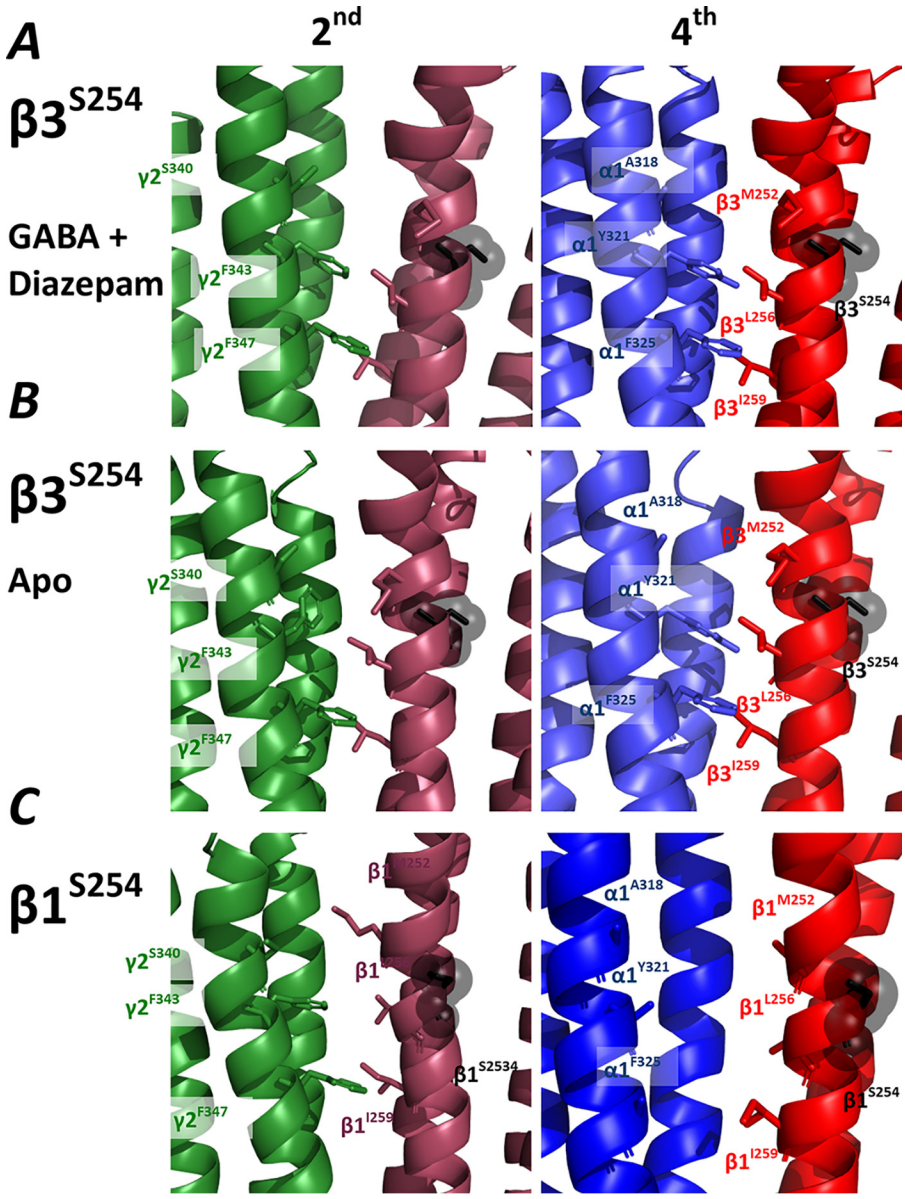

Figure 8. *A–C*, *enlarged view* of the GABA and diazepam-bound $\alpha1\beta3\gamma2$ cryo-EM structure (PDB code 6HUP) (*A*), apo-$\alpha1\beta3\gamma2$ (PDB 6i53) (*B*), and $\alpha1\beta1\gamma2$ (PDB code 6DW0) (*C*) (40, 41) showing the $\beta3^{S254}$ or $\beta1^{S254}$ mutant residues in the two different subunit locations of the second $\beta3$ subunit (*left*) and fourth $\beta3$ subunit (*right*). The subunits are *colored* with the first $\gamma2$ subunit in *green*, the second $\beta3$ subunit in *maroon*, the third $\alpha1$ subunit in *light blue*, the fourth $\beta3$ subunit in *red*, and the fifth $\alpha1$ subunit in *dark blue*. Residues from adjacent $\alpha1$ or $\gamma2$ subunits are indicated. Although the interacting partners of the Ser-254 residue are within the β subunit, the increased volume of the phenylalanine residue that substitutes for the serine at position 254 will cause the helix to occupy the space closer to the M3 helix of the adjacent subunit. When in the second position in the apo or $\alpha1\beta1\gamma2$ structures, the M3 helix of the $\gamma2$ helix is kinked rather than parallel to the M1 helix of the β subunit. The residues of the M1 and M3 that face each other are the $\beta1^{M253}$, $\beta1^{L256}$, and $\beta1^{I259}$ residues for both subunits; the $\gamma2^{V341}$, $\gamma2^{I344}$, $\gamma2^{F345}$, and $\gamma2^{S348}$ residues of the first subunit (*left*); and the $\alpha1^{Y321}$, $\alpha1^{F323}$, and $\alpha1^{Y325}$ residues of the third subunit (*right*). At the locations of all of these mutations, the sequence between $\beta1$ and $\beta3$ is identical.

The effects of the $\beta3^{S254F}$ mutation were very different, having markedly different shifts in the potency of GABA, depending on the location of the mutation. Notably, mutations in the proline residue that precedes the same serine in the $\beta1$ subunit also cause the potency of GABA to increase, but the same mutation in an $\alpha1$ subunit failed to assemble in HEK293 cells (45). Although we found robust activation of the receptors in our oocyte expression system, it is possible that the mutations also impair assembly or trafficking to the cell surface in the mammalian cell. We also cannot rule out that the mutant subunit preferentially arranges itself in the location where the potency of GABA is reduced, leading to impaired GABA activation. Importantly, we have only considered the effect of the mutation on the synaptic $\alpha1\beta3\gamma2$, and the effect of the mutation in other GABA receptor subtypes, including $\alpha5\beta3\gamma2$ or $\alpha4\beta3\delta$ receptors, may contribute to the overall phenotype, including seizures. Indeed, all $\beta3$ mutations would be expressed in these subtypes, and as such, the effects of the $\beta3^{D120N}$, $\beta3^{T157M}$, and $\beta3^{Y302C}$ on extrasynaptic receptors also need to be considered, particularly when the $\beta3^{T157M}$ mutation has been reported to have little effect when expressed in the $\alpha5\beta3\gamma2$ subtype (8). It is also possible that the $\beta3^{S254F}$ mutation is not truly pathogenic in itself; however, this mutation has been subsequently identified *de novo* in another patient and is therefore very unlikely not to be pathogenic (46).

Conclusions and future directions

Genetic epileptic encephalopathies are a devastating group of severe childhood epilepsies that are often resistant to pharmacological treatment and include patients with mutations in genes that encode for the $GABA_A$ receptor. Introducing mutations to concatenated receptors demonstrates that the number of mutations within the receptor matter. Typically, the incorporation of one mutation impairs the activation properties of the receptor, reducing the GABA potency, efficacy, or both, and the incorporation of two mutations is often catastrophic to receptor function. However, the mutations are complex, where individual mutations can also increase the potency of GABA, and the subunit location of the mutation can also determine the functional change in the mutation. The resultant molecular phenotype is likely a complex mixture of receptors with a mix of WT receptors, receptors containing a single mutation, and receptors containing two mutations. Furthermore, receptors containing one mutation that have an intermediate effect on the activation process may be a useful target for GABAergic drugs to confer the most benefit for their specific mutation.

Experimental procedures

Molecular biology

Human cDNAs for monomeric α1, β3, and γ2 $GABA_AR$ subunits were kind gifts from Saniona A/S (Copenhagen, Denmark). The γ2, β3, and α1 subunits were initially subcloned into five separate in-house vectors. Linker sequences were then added through standard PCRs, where the antisense oligonucleotides caused deletion of the stop codon and in-frame fusion to the AGS linker sequence, and the sense β3 or α1 oligonucleotides caused omission of the respective β3 or α1 signal peptide and in-frame fusion to the AGS linker sequence. The remaining sequences of the sense and antisense oligonucleotides were designed to match the respective WT sequences and included unique restriction sites within each linker region and at the beginning and end of each gene sequence. Standard PCRs with the γ2, β3, or α1 sequences as template were performed using Q5 polymerase (Genesearch, Gold Coast, Australia), and PCR products were cloned into in-house vectors using restriction enzyme digestion and ligation. Correct introduction of linker sequences and fidelity of all coding sequences were verified by double-stranded sequencing. The γ2-β3-α1-β3-α1 concatenated construct was then created by a restriction enzyme digest of the five vectors and ligation of the five subunits with linker sequences and subcloned into an in-house vector. The resulting construct contained the subunits with linker sequences in the order of γ2-$(AGS)_5$-β3-$(AGS)_5$LGS$(AGS)_3$-α1- AGT$(AGS)_5$-β3-$(AGS)_4$ATG$(AGS)_4$-α1. The vector was transformed into *Escherichia coli* 10-β bacteria for plasmid amplification, and purifications were performed with standard kits (Qiagen, Chadstone, Australia). Mutations were made using the QuikChange II site-directed mutagenesis kit (Agilent Technologies, Mulgrave, Australia) in vectors containing single subunits and flanking linker sequences and then confirmed through dsDNA sequencing. A restriction digest was then performed on subunit DNA containing the mutation and the concatenated construct to remove the appropriate WT subunit and then ligated to introduce the mutant subunit. DNA gel electrophoresis was performed to ensure incorporation of the five subunits. cRNA was produced from linearized cDNA using the mMessage mMachine T7 Transcription kit (Thermo Fisher, Scoresby, Australia) according to the manufacturer's description and stored at −80 °C until use.

Xenopus surgery and oocyte preparation

All procedures using *Xenopus laevis* frogs were approved by the animal ethics committee of the University of Sydney (AEC number 2013/5269) and are in accordance with the National Health and Medical Research Council (NHMRC) of Australia code for the care and use of animals. In brief, a section of ovarian lobe from *X. laevis* was surgically removed while the frog was under anesthesia induced by tricaine, cut into smaller portions, and digested with 35 mg of collagenase-A diluted in 15 ml of OR2 (82.5 mM NaCl, 5 mM HEPES, 2 mM $MgCl_2$, and 2 mM KCl, pH 7.4) at 18 °C for ∼1 h until the oocytes were fully detached from the follicles and the ovary tissue. Oocytes were then injected with a total of 2 ng of cRNA per cell that encoded concatenated WT or mutant receptors and were incubated for 2–4 days on an oscillator at 18 °C in ND96 solution (96 mM NaCl, 2 mM KCl, 1 mM $MgCl_2$, 1.8 mM $CaCl_2$, 5 mM HEPES, pH 7.4) supplemented with 2.5 mM pyruvate, 0.5 mM theophylline, and 50 μg/ml gentamycin.

Two-electrode voltage-clamp recording

Cell currents were recorded using the two-electrode voltage-clamp method as described previously (47). Briefly, oocytes were continuously superfused at room temperature with ND96 at ∼5 ml/min. Cells were impaled with microelectrodes fashioned from capillary glass (Harvard Apparatus, Holliston, MA) that were prepared with a micropipette puller (Narishige, Tokyo, Japan) and filled with 3 M KCl (0.3–2.0 megaohms) and then voltage-clamped at −60 mV. A semi-automated three-channel oocyte recording system was used, where the application of solution was controlled through programming of a Powerlab 8/36 data acquisition system (ADI Instruments, Sydney, Australia) that switched solutions through a VC-8 eight-channel perfusion system (Warner Instruments LLC, Hamden, CT) and then applied solution to three recording chambers. Currents were recording using a GeneClamp 500B (Axon Instruments, Foster City, CA) or OC-725C amplifier clamp (Warner Instruments) and digitized with a Powerlab 8/36 and LabChart version 8.03 (ADInstruments, Sydney, Australia).

For clobazam concentration–response curves, a 10 μM concentration was applied as a reference, and the responses were normalized to the mean current of the second two GABA concentrations. For all other experiments, a 3 mM concentration of GABA was applied as a reference three times during the experiment, and for concentration–response curves, peak currents were normalized to the mean current of the second two GABA applications. When estimating the maximal P_O, after three consecutive applications of the reference 3 mM GABA solution, the solution containing 10 mM GABA, 1 μM diazepam, and 3 μM etomidate was applied, and peak currents were normalized to the mean current of the second two GABA applications. A washout period of 10–12 min was performed between GABA

applications to prevent effects from desensitization. All experiments were performed over a minimum of two different batches of oocytes, and a minimum of 10 individual experiments were performed. The GABA applications were applied in a sequence identical to those shown in the representative data figures. Data were acquired at 1 kHz, and, for the purposes of displaying representative traces, the data were converted to 10 Hz offline through Microsoft excel.

Data analysis and statistics

Concentration–response curves were fitted using GraphPad Prism version 7 to a monophasic Hill equation of the form,

$$I = I_{max}\frac{[A]^{n_H}}{[A]^{n_H} + EC_{50}{}^{n_H}} \quad \text{(Eq. 1)}$$

where I_{max} is the maximum current, EC_{50} is the concentration that produces the half-maximum response, [A] is the concentration of ligand, and n_H is the Hill slope. Individual oocytes where a complete concentration–response curve was taken are recorded as a single *n*. Responses were normalized to the fitted maximum response of individual concentration–response curves. The EC_{50} shown is from the fitting of Hill equations to all data, whereas the log EC_{50}, I_{max}, and n_H values are the mean and S.E. derived from fitting curves to individual experiments.

For clobazam concentration–response curves, the percent modulation of clobazam was derived by the equation.

$$\text{Percent modulation} = 100 \times \frac{I_{\text{clobazam}} - I_{10\ \mu\text{M GABA}}}{I_{10\ \mu\text{M GABA}}} \quad \text{(Eq. 2)}$$

These data were then fitted to the Hill equation, as above, to determine the parameters of the concentration–response curves.

The estimated $P_{o(max)}$ for individual experiments was derived by the equation.

$$\text{Est. } P_{0(max)} = \text{correction factor} \times \frac{I_{3\ \text{mM GABA}}}{I_{10\ \text{mM GABA, }1\ \mu\text{M diazepam, }3\ \mu\text{M etomidate}}} \quad \text{(Eq. 3)}$$

The correction factor was determined for each mutation to correct for the fact that 3 mM GABA did not always elicit the maximum response to GABA. This was derived from rearranging the Hill equation,

$$\text{Correction factor} = 1 + \frac{0.003^{n_H}}{EC_{50}{}^{n_H}} \quad \text{(Eq. 4)}$$

where the EC_{50} was in M.

When comparing the WT and mutation concentration–response curves, all data were transformed to the Est. $P_{o(max)}$.

For statistical analysis, Est. $P_{o(max)}$ values and parameters derived from concentration–response curves were compared with a one-way ANOVA with Tukey's post hoc test. Significance values of $p < 0.05$, $p < 0.01$, and $p < 0.001$ are shown under "Results."

Author contributions—N. L. A., P. K. A., J. C. A., I. S. M., M. T. B., and M. C. conceptualization, N. L. A. data curation; N. L. A., T. B., and T. J. formal analysis; N. L. A., P. K. A., T. B., T. J., L. L. A., and M. C. investigation; N. L. A., P. K. A., V. W. L., T. B., T. J., and L. L. A. methodology; N. L. A., M. T. B., and M. C. writing-original draft; N. L. A., J. C. A., I. S. M., M. T. B., and M. C. project administration; N. L. A., P. K. A., V. W. L., T. B., J. C. A., I. S. M., M. T. B., and M. C. writing-review and editing; P. K. A., V. W. L., and T. B. resources; J. C. A., I. S. M., M. T. B., and M. C. funding acquisition; M. C. supervision.

References

1. Howard, M. A., and Baraban, S. C. (2017) Catastrophic epilepsies of childhood. *Annu. Rev. Neurosci.* **40,** 149–166 CrossRef Medline
2. Cossette, P., Liu, L., Brisebois, K., Dong, H., Lortie, A., Vanasse, M., Saint-Hilaire, J. M., Carmant, L., Verner, A., Lu, W. Y., Wang, Y. T., and Rouleau, G. A. (2002) Mutation of GABRA1 in an autosomal dominant form of juvenile myoclonic epilepsy. *Nat. Genet.* **31,** 184–189 CrossRef Medline
3. Gontika, M. P., Konialis, C., Pangalos, C., and Papavasiliou, A. (2017) Novel *SCN1A* and *GABRA1* gene mutations with diverse phenotypic features and the question on the existence of a broader spectrum of Dravet syndrome. *Child Neurol. Open* **4,** 2329048X17706794 CrossRef Medline
4. Hernandez, C. C., Klassen, T. L., Jackson, L. G., Gurba, K., Hu, N., Noebels, J. L., and Macdonald, R. L. (2016) Deleterious rare variants reveal risk for loss of GABA$_A$ receptor function in patients with genetic epilepsy and in the general population. *PLoS One* **11,** e0162883 CrossRef Medline
5. Johannesen, K., Marini, C., Pfeffer, S., Møller, R. S., Dorn, T., Niturad, C. E., Gardella, E., Weber, Y., Søndergård, M., Hjalgrim, H., Nikanorova, M., Becker, F., Larsen, L. H., Dahl, H. A., Maier, O., *et al.* (2016) Phenotypic spectrum of GABRA1: from generalized epilepsies to severe epileptic encephalopathies. *Neurology* **87,** 1140–1151 CrossRef Medline
6. Kodera, H., Ohba, C., Kato, M., Maeda, T., Araki, K., Tajima, D., Matsuo, M., Hino-Fukuyo, N., Kohashi, K., Ishiyama, A., Takeshita, S., Motoi, H., Kitamura, T., Kikuchi, A., Tsurusaki, Y., *et al.* (2016) *De novo* GABRA1 mutations in Ohtahara and West syndromes. *Epilepsia* **57,** 566–573 CrossRef Medline
7. Lachance-Touchette, P., Brown, P., Meloche, C., Kinirons, P., Lapointe, L., Lacasse, H., Lortie, A., Carmant, L., Bedford, F., Bowie, D., and Cossette, P. (2011) Novel α1 and γ2 GABA$_A$ receptor subunit mutations in families with idiopathic generalized epilepsy. *Eur. J. Neurosci.* **34,** 237–249 CrossRef Medline
8. Møller, R. S., Larsen, L. H., Johannesen, K. M., Talvik, I., Talvik, T., Vaher, U., Miranda, M. J., Farooq, M., Nielsen, J. E., Svendsen, L. L., Kjelgaard, D. B., Linnet, K. M., Hao, Q., Uldall, P., Frangu, M., *et al.* (2016) Gene panel testing in epileptic encephalopathies and familial epilepsies. *Mol. Syndromol.* **7,** 210–219 CrossRef Medline
9. Stosser, M. B., Lindy, A. S., Butler, E., Retterer, K., Piccirillo-Stosser, C. M., Richard, G., and McKnight, D. A. (2018) High frequency of mosaic pathogenic variants in genes causing epilepsy-related neurodevelopmental disorders. *Genet. Med.* **20,** 403–410 CrossRef Medline
10. Epi4K Consortium, Epilepsy Phenome/Genome Project, Allen, A. S., Berkovic, S. F., Cossette, P., Delanty, N., Dlugos, D., Eichler, E. E., Epstein, M. P., Glauser, T., Goldstein, D. B., Han, Y., Heinzen, E. L., Hitomi, Y., Howell, K. B., *et al.* (2013) *De novo* mutations in epileptic encephalopathies. *Nature* **501,** 217–221 CrossRef Medline
11. Janve, V. S., Hernandez, C. C., Verdier, K. M., Hu, N., and Macdonald, R. L. (2016) Epileptic encephalopathy de novo GABRB mutations impair GABAA receptor function. *Ann. Neurol.* **79,** 806–825 CrossRef Medline
12. Papandreou, A., McTague, A., Trump, N., Ambegaonkar, G., Ngoh, A., Meyer, E., Scott, R. H., and Kurian, M. A. (2016) GABRB3 mutations: a new and emerging cause of early infantile epileptic encephalopathy. *Dev. Med. Child. Neurol.* **58,** 416–420 CrossRef Medline
13. Baulac, S., Huberfeld, G., Gourfinkel-An, I., Mitropoulou, G., Beranger, A., Prud'homme, J. F., Baulac, M., Brice, A., Bruzzone, R., and LeGuern, E. (2001) First genetic evidence of GABA$_A$ receptor dysfunction in epilepsy:

a mutation in the γ2-subunit gene. *Nat. Genet.* **28,** 46–48 CrossRef Medline

14. Boillot, M., Morin-Brureau, M., Picard, F., Weckhuysen, S., Lambrecq, V., Minetti, C., Striano, P., Zara, F., Iacomino, M., Ishida, S., An-Gourfinkel, I., Daniau, M., Hardies, K., Baulac, M., Dulac, O., *et al.* (2015) Novel GABRG2 mutations cause familial febrile seizures. *Neurol. Genet.* **1,** e35 CrossRef Medline
15. Shen, D., Hernandez, C. C., Shen, W., Hu, N., Poduri, A., Shiedley, B., Rotenberg, A., Datta, A. N., Leiz, S., Patzer, S., Boor, R., Ramsey, K., Goldberg, E., Helbig, I., Ortiz-Gonzalez, X. R., *et al.* (2017) *De novo* GABRG2 mutations associated with epileptic encephalopathies. *Brain* **140,** 49–67 CrossRef Medline
16. Wallace, R. H., Marini, C., Petrou, S., Harkin, L. A., Bowser, D. N., Panchal, R. G., Williams, D. A., Sutherland, G. R., Mulley, J. C., Scheffer, I. E., and Berkovic, S. F. (2001) Mutant GABA$_A$ receptor γ2-subunit in childhood absence epilepsy and febrile seizures. *Nat. Genet.* **28,** 49–52 CrossRef Medline
17. Khazipov, R. (2016) GABAergic synchronization in epilepsy. *Cold Spring Harb. Perspect. Med.* **6,** a022764 CrossRef Medline
18. Miller, P. S., and Aricescu, A. R. (2014) Crystal structure of a human GABA$_A$ receptor. *Nature* **512,** 270–275 CrossRef Medline
19. Olsen, R. W. (2018) GABA$_A$ receptor: positive and negative allosteric modulators. *Neuropharmacology* **136,** 10–22 CrossRef Medline
20. Hevers, W., and Lüddens, H. (1998) The diversity of GABA$_A$ receptors: pharmacological and electrophysiological properties of GABAA channel subtypes. *Mol. Neurobiol.* **18,** 35–86 CrossRef Medline
21. Farrant, M., and Nusser, Z. (2005) Variations on an inhibitory theme: phasic and tonic activation of GABA$_A$ receptors. *Nat. Rev. Neurosci.* **6,** 215–229 CrossRef Medline
22. Bouzat, C. (2012) New insights into the structural bases of activation of Cys-loop receptors. *J. Physiol. Paris* **106,** 23–33 CrossRef Medline
23. Ahring, P. K., Liao, V. W. Y., and Balle, T. (2018) Concatenated nicotinic acetylcholine receptors: a gift or a curse? *J. Gen. Physiol.* **150,** 453 CrossRef Medline
24. Baumann, S. W., Baur, R., and Sigel, E. (2002) Forced subunit assembly in alpha1beta2gamma2 GABAA receptors: insight into the absolute arrangement. *J. Biol. Chem.* **277,** 46020–46025 CrossRef Medline
25. Sigel, E., Kaur, K. H., Lüscher, B. P., and Baur, R. (2009) Use of concatamers to study GABAA receptor architecture and function: application to δ-subunit-containing receptors and possible pitfalls. *Biochem. Soc. Trans.* **37,** 1338–1342 CrossRef Medline
26. Baur, R., Minier, F., and Sigel, E. (2006) A GABA$_A$ receptor of defined subunit composition and positioning: concatenation of five subunits. *FEBS Lett.* **580,** 1616–1620 CrossRef Medline
27. Ramerstorfer, J., Furtmüller, R., Sarto-Jackson, I., Varagic, Z., Sieghart, W., and Ernst, M. (2011) The GABA$_A$ receptor α+β-interface: a novel target for subtype selective drugs. *J. Neurosci.* **31,** 870–877 CrossRef Medline
28. Che Has, A. T., Absalom, N., van Nieuwenhuijzen, P. S., Clarkson, A. N., Ahring, P. K., and Chebib, M. (2016) Zolpidem is a potent stoichiometry-selective modulator of α1β3 GABAA receptors: evidence of a novel benzodiazepine site in the α1-α1 interface. *Sci. Rep.* **6,** 28674 CrossRef Medline
29. Hammer, H., Ebert, B., Jensen, H. S., and Jensen, A. A. (2015) Functional characterization of the 1,5-benzodiazepine clobazam and its major active metabolite *N*-desmethylclobazam at human GABA$_A$ receptors expressed in *Xenopus laevis* oocytes. *PLoS One* **10,** e0120239 CrossRef Medline
30. Shin, D. J., Germann, A. L., Johnson, A. D., Forman, S. A., Steinbach, J. H., and Akk, G. (2018) Propofol is an allosteric agonist with multiple binding sites on concatemeric ternary GABA$_A$ receptors. *Mol. Pharmacol.* **93,** 178–189 CrossRef Medline
31. Fisher, J. L., and Macdonald, R. L. (1997) Single channel properties of recombinant GABA$_A$ receptors containing γ2 or δ subtypes expressed with α1 and β3 subtypes in mouse L929 cells. *J. Physiol.* **505,** 283–297 CrossRef Medline
32. Purohit, P., Gupta, S., Jadey, S., and Auerbach, A. (2013) Functional anatomy of an allosteric protein. *Nat. Commun.* **4,** 2984 CrossRef Medline
33. Kash, T. L., Dizon, M. J., Trudell, J. R., and Harrison, N. L. (2004) Charged residues in the β2 subunit involved in GABA$_A$ receptor activation. *J. Biol. Chem.* **279,** 4887–4893 CrossRef Medline
34. Kash, T. L., Jenkins, A., Kelley, J. C., Trudell, J. R., and Harrison, N. L. (2003) Coupling of agonist binding to channel gating in the GABA$_A$ receptor. *Nature* **421,** 272–275 CrossRef Medline
35. Sigel, E., and Steinmann, M. E. (2012) Structure, function, and modulation of GABA$_A$ receptors. *J. Biol. Chem.* **287,** 40224–40231 CrossRef Medline
36. Ahring, P. K., Bang, L. H., Jensen, M. L., Strøbaek, D., Hartiadi, L. Y., Chebib, M., and Absalom, N. (2016) A pharmacological assessment of agonists and modulators at α4β2γ2 and α4β2δ GABAA receptors: the challenge in comparing apples with oranges. *Pharmacol. Res.* **111,** 563–576 CrossRef Medline
37. Lape, R., Colquhoun, D., and Sivilotti, L. G. (2008) On the nature of partial agonism in the nicotinic receptor superfamily. *Nature* **454,** 722–727 CrossRef Medline
38. Sigel, E., Baur, R., Boulineau, N., and Minier, F. (2006) Impact of subunit positioning on GABAA receptor function. *Biochem. Soc. Trans.* **34,** 868–871 CrossRef Medline
39. Gallagher, M. J., Song, L., Arain, F., and Macdonald, R. L. (2004) The juvenile myoclonic epilepsy GABA$_A$ receptor α1 subunit mutation A322D produces asymmetrical, subunit position-dependent reduction of heterozygous receptor currents and α1 subunit protein expression. *J. Neurosci.* **24,** 5570–5578 CrossRef Medline
40. Phulera, S., Zhu, H., Yu, J., Claxton, D. P., Yoder, N., Yoshioka, C., and Gouaux, E. (2018) Cryo-EM structure of the benzodiazepine-sensitive α1β1γ2S tri-heteromeric GABAA receptor in complex with GABA. *Elife* **7,** e39383 CrossRef Medline
41. Laverty, D., Desai, R., Uchański, T., Masiulis, S., Stec, W. J., Malinauskas, T., Zivanov, J., Pardon, E., Steyaert, J., Miller, K. W., and Aricescu, A. R. (2019) Cryo-EM structure of the human α1β3γ2 GABA$_A$ receptor in a lipid bilayer. *Nature* **565,** 516–520 CrossRef Medline
42. Absalom, N. L., Lewis, T. M., and Schofield, P. R. (2004) Mechanisms of channel gating of the ligand-gated ion channel superfamily inferred from protein structure. *Exp. Physiol.* **89,** 145–153 CrossRef Medline
43. Wood, J. D. (1975) The role of γ-aminobutyric acid in the mechanism of seizures. *Prog. Neurobiol.* **5,** 77–95 CrossRef Medline
44. Kang, J. Q., Shen, W., Zhou, C., Xu, D., and Macdonald, R. L. (2015) The human epilepsy mutation GABRG2(Q390X) causes chronic subunit accumulation and neurodegeneration. *Nat. Neurosci.* **18,** 988–996 CrossRef Medline
45. Greenfield, L. J., Jr, Zaman, S. H., Sutherland, M. L., Lummis, S. C., Niemeyer, M. I., Barnard, E. A., and Macdonald, R. L. (2002) Mutation of the GABAA receptor M1 transmembrane proline increases GABA affinity and reduces barbiturate enhancement. *Neuropharmacology* **42,** 502–521 CrossRef Medline
46. Liu, J., Tong, L., Song, S., Niu, Y., Li, J., Wu, X., Zhang, J., Zai, C. C., Luo, F., Wu, J., Li, H., Wong, A. H. C., Sun, R., Liu, F., and Li, B. (2018) Novel and *de novo* mutations in pediatric refractory epilepsy. *Mol. Brain* **11,** 48 CrossRef Medline
47. Chua, H. C., Absalom, N. L., Hanrahan, J. R., Viswas, R., and Chebib, M. (2015) The direct actions of GABA, 2′-methoxy-6-methylflavone and general anaesthetics at β3γ2L GABA$_A$ receptors: evidence for receptors with different subunit stoichiometries. *PLoS One* **10,** e0141359 CrossRef Medline